STUDIES IN VIBRATIONAL SPECTROSCOPY

I. NORMAL COORDINATE ANALYSIS OF CF_3OF AND CF_3OCl

II. RAMAN SPECTRA OF $CF_2(OF)_2$ AS A FUNCTION OF
    TEMPERATURE

by

JENG-CHUNG KUO

B.S., National Taiwan University, 1972

————————————

A MASTER'S THESIS

Submitted in partial fulfillment of the

requirements for the degree

MASTER OF SCIENCE

Department of Chemistry

KANSAS STATE UNIVERSITY
Manhattan, Kansas

1978

Approved by:

R. M. Hammaker

Major Professor

TABLE OF CONTENTS

PART   II

RAMAN SPECTRA OF $CF_2(OF)_2$ AS A FUNCTION OF TEMPERATURE

LIST OF TABLES

PART I

NORMAL COORDINATE ANALYSIS OF CF_3OF AND CF_3OCl

Table   Page

PART II

RAMAN SPECTRA OF $CF_2(OF)_2$ AS A FUNCTION OF TEMPERATURE

LIST OF FIGURES

PART I

NORMAL COORDINATE ANALYSIS OF CF_3OF AND CF_3OCl

PART II

RAMAN SPECTRA OF $CF_2(OF)_2$ AS A FUNCTION OF TEMPERATURE

I. NORMAL COORDINATE ANALYSIS OF CF_3OF and CF_3OCl

CHAPTER I
INTRODUCTION AND STATEMENT OF PROBLEM

Normal coordinate analyses relate the observed, or preferably the harmonic, infrared and Raman vibrational frequencies to the force constants, equilibrium geometry, and atomic masses of the oscillating system (1). The development of increasingly reliable intramolecular force fields for a wide variety of molecules suggests that judicious applications of normal coordinate analyses may serve as an additional means for confidently probing the structural and bonding characteristics of diverse chemical systems.

For interpreting the vibrational spectra of larger systems, the concepts of modified potential functions and of the transferability of selected force constants from chemically similar but smaller molecules emerge.

The present study consists of two separate parts. The first part is a detailed study of the normal coordinate analyses of CF_3OX (X=F, Cl) compounds. These two compounds are of interest because they are the initial members of the respective R_fOF and R_fOCl series, where R_f denotes the perfluoroalkyl group (2,3). The second part deals with the Raman spectrum of $CF_2(OF)_2$ and is discussed later in the thesis.

Our purpose in this part is twofold. The first objective

2

is to evaluate some results of previous vibrational analyses (4,5). With the complete analyses of the CF_3OX series, we will be able to see whether or not the vibrational frequencies chosen for fundamentals can be fitted reasonably well with a realistic potential function. Success in fitting the assignment with a realistic potential function will serve as evidence for the reliability of the new assignments which in turn may clarify some questionable results reported by Wilt and Jones (4) and support the work of Smardzewski and Fox (5) and of Buckley and Weber (6).

The second objective is to use the result of the CF_3OX series as the basis for later normal coordinate analyses of the CF_3OOX (X=H,D,F and Cl) series, where electron diffraction data are now available (7), and to assist in the assignment of CF_3OOX series members which are isoelectronic with CF_3OF and CF_3OCl (8).

In the present investigation, the calculations were carried out using the Wilson FG matrix method (9) with the computer programs written by Schachtschneider (10). Frequencies were given the weight $1/(\lambda_i)^2$, where $\lambda = 4\pi^2 c^2 \nu^2$, in the least squares fit for the CF_3OX series.

Trifluoromethyl hypofluorite (CF_3OF) is an important reagent in the synthesis of organic and inorganic fluorine compounds (2). There have been some serious spectroscopic studies of this compound since it was first prepared by

Kellog and Cady (11). This compound has been studied by in-
frared and Raman spectroscopy (4, 12), electron diffraction
(13), and microwave spectroscopy (6). Recently Raman spectra
have been obtained for CF_3OF in the gas phase as well as
diluted in argon matrices at $8^\circ K$ (5).

A force constant calculation has been performed by Wilt
and Jones based on their assignment and assumed bond lengths
and interbond angles (4). This result may not be reliable
mainly because of questionable assignments which will be
discussed below.

For the OF and CO stretches, Wilt and Jones assigned
947 cm^{-1} and 882 cm^{-1}, respectively. After performing their
study of CF_3OF and CF_3OCl in argon matrices at $8^\circ K$, Smardzewski
and Fox (5) proposed that these assignments should be reversed.
Their new assignments were based on the relative frequencies
shift for the CO and OX stretches when going from hypofluorite
to hypochlorite. The observation of a shoulder assignable to
$Cl(37)/Cl(35)$ isotopic splitting on the band assigned to the
OCl stretch in CF_3OCl supported the new assignment.

A torsional frequency of 56 cm^{-1} was assigned and used
to calculate the barrier to internal rotation of the CF_3
rotor (4). There are some discrepancies between Wilt and
Jones' infrared data and ours in the 300 cm^{-1} to 200 cm^{-1}
region. Since our Raman data are consistent with our IR data,
we must question the authenticity of the far infrared data

reported by Wilt and Jones including the 56 cm^{-1} band.

The potential barrier of 395 cm^{-1} (1.13 kcal/mole)
obtained by Wilt and Jones from the 56 cm^{-1} band was some-
what lower than the electron diffraction result of 2.5 $\pm$ 0.5
kcal/mole (13) and much lower than the microwave result of
3.9 kcal/mole (6) which corresponds to a torsional frequency
of approximately 120 cm^{-1}. A weak band centered at 126.9 cm^{-1}
was observed in the gas phase Raman spectrum of CF_3OF (5).
The assignment of this frequency as the CF_3 torsional mode
is the most reasonable choice.

Trifluoromethyl hypochlorite (CF_3OCl) is the first
member of the chloroxy perfluoroalkane series. Molecules
known to readily undergo free-radical reactions were very
effective in forming derivatives of CF_3OCl in which the
CF_3O group is retained (3). The potential of using this
compound as a reagent in the syntheses of fluorine compounds
is currently being investigated (14).

The preparation, identification and characterization
of CF_3OCl were reported almost simultaneously by two separate
group in 1968 and 1969 (3,15). The vibrational assignments
were based on infrared spectra only and the main purpose
was for characterization. The OCl stretching frequency was
assigned differently by these two groups. Both 665 cm^{-1} (15)
and 789 cm^{-1} (3) have been assigned to this mode.

Recently the complementary Raman spectra of CF_3OCl

isolated in an argon matrix at 8° K was reported (5). The band at 782.7 cm^{-1} was assigned to the OCl stretching mode of $CF_3O^{35}Cl$ on the basis of a low frequency shoulder assignable to the OCl stretching mode of $CF_3O^{37}Cl$.

No electron diffraction or microwave data for CF_3OCl have been published to the best of our knowledge. No previous attempt to do a normal coordinate analysis of this compound has been published to the best of our knowledge.

CHAPTER II
EXPERIMENTAL SECTION

A. Recording of Spectra

1. Materials

Both compounds used in this study were supplied by
Dr. D. D. DesMarteau of the Chemistry Department at Kansas
State University. CF_3OF was prepared by a similar method to
that described in the literature (16). This method involves
the cesium fluoride catalyzed addition of fluorine across the
carbon- oxygen double bond of COF_2. CF_3OCl was prepared using
the same method except that ClF was used in place of F_2.

2. Infrared Instrumentation

Survey and higher resolution spectra from 4000 to 160
cm^{-1} were obtained with a Perkin-Elmer Model 180 infrared
spectrophotometer. Instrument frequency calibration was
achieved using known absorption frequencies of polyethylene,
teflon, atmospheric water and CO_2 (17).

Infrared spectra of the vapor were recorded in 10 and
15 cm cells made of Pyrex tubing and a 5 cm cell made of
stainless steel. The 15 cm cell with polyethylene windows
was used for far-infrared spectra, while the 5 cm and 10 cm
cell with AgCl windows were used for the mid-range infrared
region.

3. Raman Instrumentation

The liquid Raman spectra were recorded in a low tempera-

ture cell similar in design to that of Brown et.al. (18)
using a JASCO R-300 Laser Raman Spectrophotometer and the
5145 Å line of a Spectra-Physics Model 164-00 argon ion laser.

The gaseous Raman spectra were recorded at the U. S.
Naval Research Laboratory using a Jarrel-Ash Model 500
½-meter double monochromator and the 4880 and 5145 Å lines
of a Spectra-Physics Model 164-00 argon ion laser (19).

B. Computer Programs

Several computer programs for the normal coordinate
analysis of molecular vibration are available. The ones used
in this work are from the set written by Schachtschneider
(10).

The programs, CART, GMAT, FPERT and VSEC comprise the
package of computer programs selected to fit our needs.
CART and GMAT are designed for setting up the vibrational
secular equation while VSEC and FPERT are designed for
solving the secular equation. FPERT also provides for the
least-square refinement of force constants.

CART calculates the Cartesian coordinates of the atoms
in a molecule from the bond distances and bond angles. Center
of mass and moments of intertia can also be computed. If
desired, the principal moments of inertia and the principal
Cartesian coordinates are also calculated.

GMAT calculates the Wilson G matrix (i.e., the vibra-
tional inverse kinetic energy matrix) for polyatomic mole-
cules. Input for this program are the Cartesian coordinates
(from the output of CART), masses of the atoms, the numbers
of the atoms defining a complete set of internal valence
coordinates (i.e., bond stretching, valence angle bending,
out-of-plane wagging and torsion) (10,20) and the transfor-
mation to symmetry coordinates if desired.

VSEC solves the secular equations in internal coordinates
by two successive Jacobi diagonalizations. Factoring of the
secular equation can be carried out within the program. At
the option of the user the mean amplitudes of vibration, the
eigenvector inverse matrix L^{-1}, and Coriolis coefficients
may be calculated.

FPERT refines a set of force constants to give a weighted
least-squares fit between observed and calculated frequencies.
The secular equation in the first cycle is solved in internal
coordinates by two successive Jacobi diagonalizations.

All the programs are coded in Fortran IV language.
Standarized input-output formats are used so the same cards
can be used in all programs.

CHAPTER III
EXPERIMENTAL RESULTS

In this chapter the experimental spectroscopic data for CF_3OF and CF_3OCl are presented. Summaries derived from both infrared and Raman data are made for both molecules. Only frequencies in the fundamental region (below 1400 cm^{-1}) are included in the summaries.

A.   Infrared Spectra of CF_3OF

A summary of the infrared data below 1400 cm^{-1} is presented in Table 1. The gas-phase infrared spectra of CF_3OF in the fundamental region 1400-200 cm^{-1} are shown in Figures 1 and 2. A 10X abscissa scale expansion of the 429 cm^{-1} band is also shown at the top of Figure 2. A shoulder at 431 cm^{-1} is observed. This shoulder was first neglected but finally assigned as a fundamental as suggested by the normal coordinate analysis. In general the infrared data presented agree well with that of Wilt and Jones (4). Between 300 and 200 cm^{-1} our spectra differ from those of Wilt and Jones in that our peaks are 25-28 cm^{-1} higher in frequencies although the band shapes are somewhat similar.

B.   Raman Spectra of CF_3OF

The low and high sensitivity Raman spectra of CF_3OF near $-196^\circ C$ are shown in Figures 3 and 4, respectively. A reduced scale Raman gas phase spectrum of CF_3OF, which was provided by Drs. R. R. Smardzewski and W. B. Fox of the

U. S. Naval Research Laboratory, Washington, D. C., is also shown in Figure 3. Experimental conditions including the laser source and temperature are included with each spectrum. Table 1 lists the gas, liquid, and Ar matrix Raman frequencies and the assignments made in this study are also included.

C. Infrared Spectra of CF_3OCl

The infrared spectrum in the fundamental region from 1400 cm^{-1} to 180 cm^{-1} in the gas phase is shown in Figures 5 and 6. A summary is in Table 2. The general appearance of the infrared spectrum is very similar to that of Schack and Maya (3). However, the region below 500 cm^{-1} was not included in their report.

D. Raman Spectra of CF_3OCl

The low and high sensitivity Raman spectra of liquid CF_3OCl at $-196^\circ C$ are shown in Figures 7 and 8. The band at 548 cm^{-1}, which is very prominent on the side of the 561 cm^{-1} band in the liquid Raman spectrum but completely absent in the IR spectrum, is attributed to residual chlorine complexed with CF_3OCl. Table 2 lists the liquid and Ar matrix Raman frequencies and the assignments made in this study are also included.

E. Matrix Spectra of Smardzewski and Fox (5)

Figure 9A illustrates the spectral region containing the $v(OX)$ and $v(CO)$ fundamentals. The complementary matrix infrared spectra are illustrated in the top portions of the

figure. It can readily be seen that the higher frequency band, which is assigned to $\nu(CO)$, undergoes a relatively minor shift (25.8 cm^{-1}) on proceeding from CF_3OF to CF_3OCl while the lower frequency band, which is assigned to $\nu(OX)$, experiences a marked decrease in frequency (99.9 cm^{-1}). Also the chlorine isotopic splitting of the 782.7 cm^{-1} matrix Raman band is shown in Figure 9B. The splitting and intensity ratio support the assignment of $\nu(OCl)$ based on frequency shift. The spectra in Figure 9 are taken from Reference (5).

Table 1.   Raman and Infrared Data for CF_3OF below 1400 cm^{-1}

Gas Raman[a]	IR[b]	Liquid Raman[b]	ρ[c]	Ar Matrix Raman[a]	Assignment[d]
1300	1294	1310		1288	a. ν_{CF_3} (A')
1250	1261			1250	a. ν_{CF_3}(A")
1219	1222	1205	0.45	1211	s. ν_{CF_3}
945	947(Q)[e]	946	0.49	945	ν_{CO}
881	882(Q)[e]	882	0.03	883	ν_{OF}
864		868	0.04	871	2 δ_{COF}
675	678(Q)[e]	679	0.035	678	s. δ_{CF_3}
606	607	609	0.85	606	a. δ_{CF_3}(A")
581	585	587	0.43	582	a. δ_{CF_3}(A')
	431 sh				ρ_{CF_3}(A")
429	429(Q)[e]	436	0.32	433	δ_{COF}
272	278	285??			$\{\,$ 2 τ_{CF_3} and
246	252	259	0.52	256	ρ_{CF_3}(A')
127	-	144	0.86	-	τ_{CF_3}

a.   References (5) and (19).

b.   D. D. DesMarteau and R. M. Hammaker unpublished studies.

c.   These depolarization ratios for the liquids were measured by rotating the polarization of the incident laser beam with no analyzer and no scrambler in the scattered beam. Known depolarized bands below 500 cm^{-1} gave depolarization ratios between 0.75 and 0.89 with this arrangement. This arrangement is method IV in H. H. Classen, H. Selig, and J. Shamir, Appl. Spectroscopy, 23. 8, (1969).

d.   These symbols refer to the work descriptions of the symmetry coordinates defined in Table 4 and of the fundamental vibrations in Table 6.

e.   These are Q branches for bands having PQR structure as follows: 938, 947, 956; 974, 882, 890; 670, 678, 688; 420, 429, 439.

EXPLANATION OF FIGURE 1

Gas-phase Infrared Spectra of CF_3OF in the Region 1400-500 cm^{-1}.

Spectrometer: Perkin-Elmer Model 180

Sampling Method: 10 cm Path Length Cell with

AgCl Windows

Pressure: Spectrum A - 3 mm Hg

Spectrum B - 161 mm Hg

Energy Mode: Constant I_o

Resolution: Spectrum A - 1.1 cm^{-1} at 1400 cm^{-1}

Spectrum B - 1.0 cm^{-1} at 1000 cm^{-1}

Gain: 6

Slit Program: 5

Time Constant: 1

Scan Time: Fine 5, Coarse 10

Suppression: 5

Temperature: 25° C
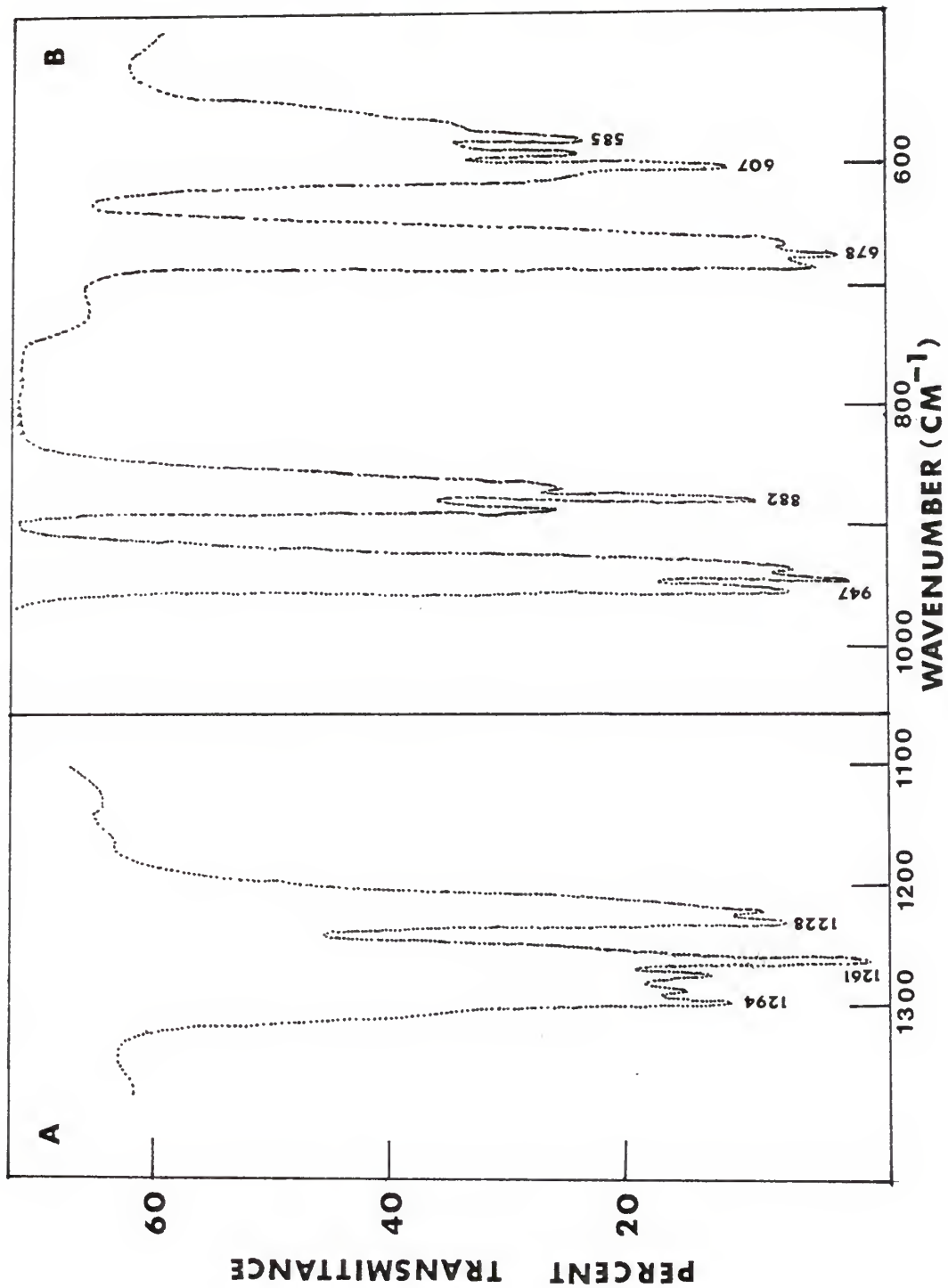
EXPLANATION OF FIGURE 2

Gas-phase Infrared Spectra of CF_3OF in the Region 650-200 cm^{-1}.

Spectrometer: Perkin-Elmer Model 180

Sampling Method: 15 cm Path Length Cell with
                 Polyethylene Windows

Pressure: 438 mm Hg

Energy Mode: Constant I_o

Resolution: 3.0 cm^{-1} at 650 cm^{-1}

Gain: 6

Slit Program: 5

Time Constant: 1

Scan Time: Fine 5, Coarse 10

Suppression: 5

Temperature: 25^oC

A 10X abscissa scale expansion of the 429 cm^{-1} band is shown directly above. A shoulder at 431 cm^{-1} is observed.

EXPLANATION OF FIGURE 3

A. Raman Spectrum of Liquid CF_3OF

Spectrometer: JASCO Model R-300

Slit Setting: 150 μm

Sensitivity: 1

Response: 0.5 Seconds

Scan Rate: 4

Power: 140 mW

Source: Ar^+ Laser at 5145 $\mathring{A}$

Temperature: -196°C

B. Raman Spectrum of Gaseous CF_3OF
(Courtesy of Dr. Richard R. Smardzewski of
Naval Research Laboratory (19))

Spectrometer: Jarrel-Ash Model 500

Slit Setting: 100 μm

Concentration: 150 mm Hg

Sensitivity: 800

Time Constant: 1 Second

Scan Rate: 2.5 cm/sec

Source: Ar^+ Laser at 5145 $\mathring{A}$

Power: 1.5 W

Temperature: 25°C
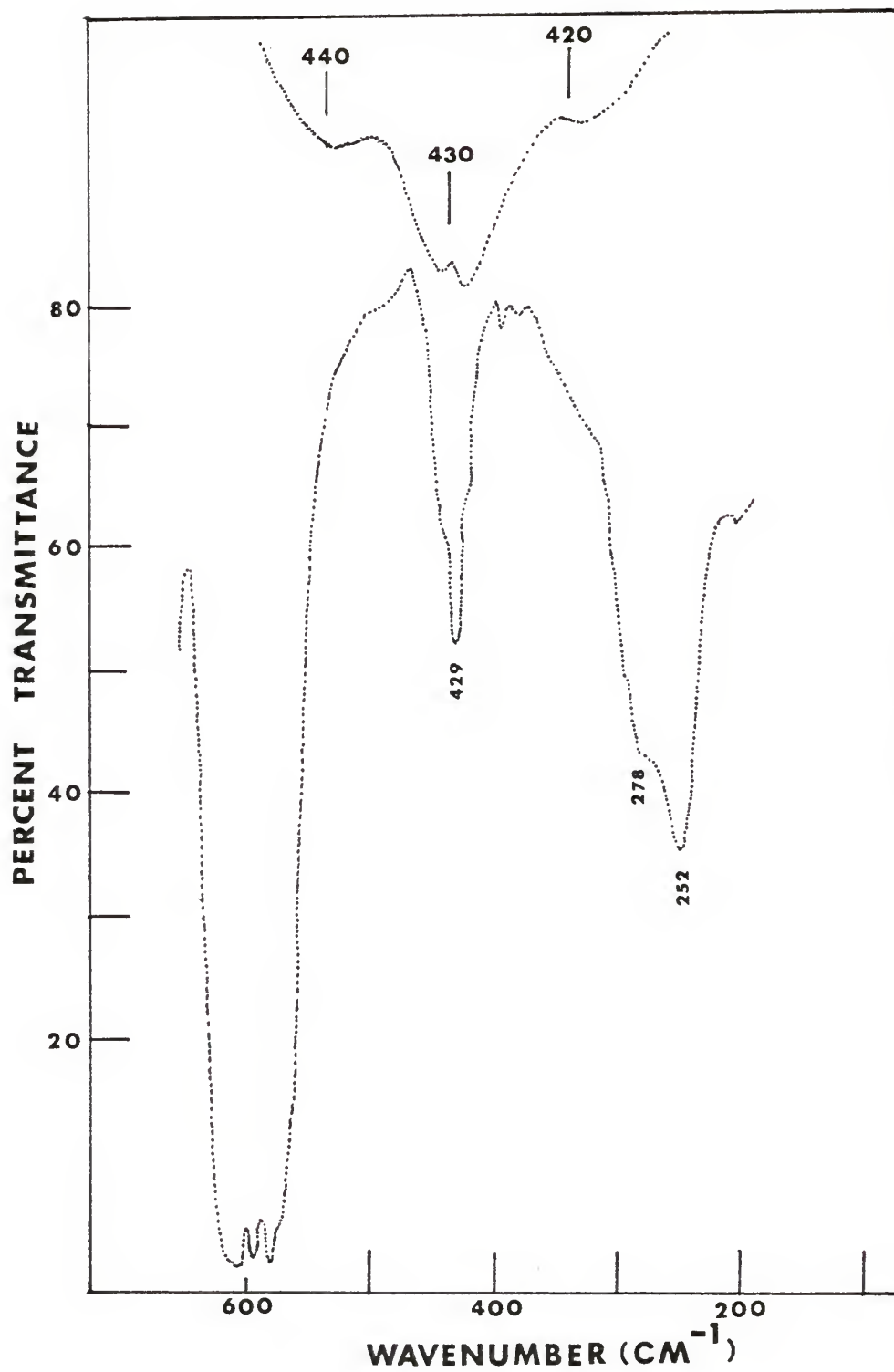
EXPLANATION OF FIGURE 4

High Sensitivity Raman Spectra of Liquid CF_3OF

Spectrometer: JASCO Model R-300

Slit Setting: 150 μm

Sensitivity: 5

Response: 2 Seconds

Scan Rate: 4

Source: Ar^+ Laser at 5145 Å

Power: 140 mW

Temperature: $-196^{\circ}C$

EXPLANATION OF FIGURE 5

Gas-phase Infrared Spectra of CF_3OCl in the Region 1400-500 cm^{-1}.

Spectrometer: Perkin-Elmer Model 180

Sampling Method: 10 cm Path Length Cell with

                AgCl Windows

Pressure: Spectrum A - 3 mm Hg

         Spectrum B - 65 mm Hg

Energy Mode: Constant I_o

Resolution: Spectrum A - 1.7 cm^{-1} at 1300 cm^{-1}

          Spectrum B - Slit width 0.2 mm at 4000 cm^{-1}

Gain: 6

Slit Program: 5

Time Constant: 1

Scan Time: Fine 5, Coarse 10

Suppression: 5

Temperature: $25^{o}C$

18
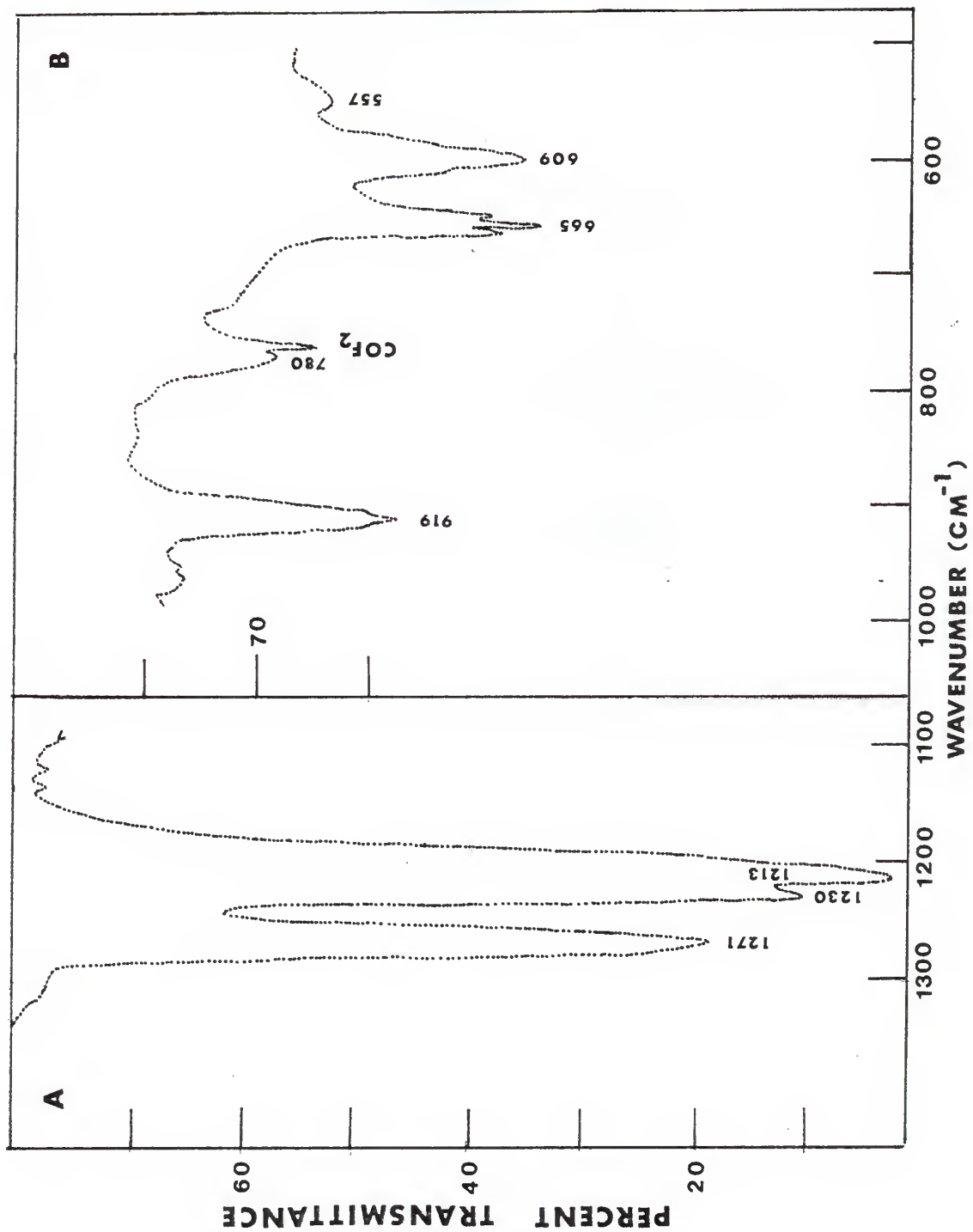
EXPLANATION OF FIGURE 6

Gas-phase Infrared Spectra of CF_3OCl in the Region 650-180 cm^{-1}.

Spectrometer: Perkin-Elmer Model 180

Sampling Method: 15 cm Path Length Cell with
                 Polyethylene Windows

Pressure: Spectrum A - 100 mm Hg
          Spectrum B - 140 mm Hg

Energy Mode: Constant I_o

Resolution: Spectrum A - 3.4 cm^{-1} at 650 cm^{-1}
            Spectrum B - 2.0 cm^{-1} at 300 cm^{-1}

Gain: 6

Slit Program: 5

Scan Time: Fine 5, Coarse 10

Suppression: 5
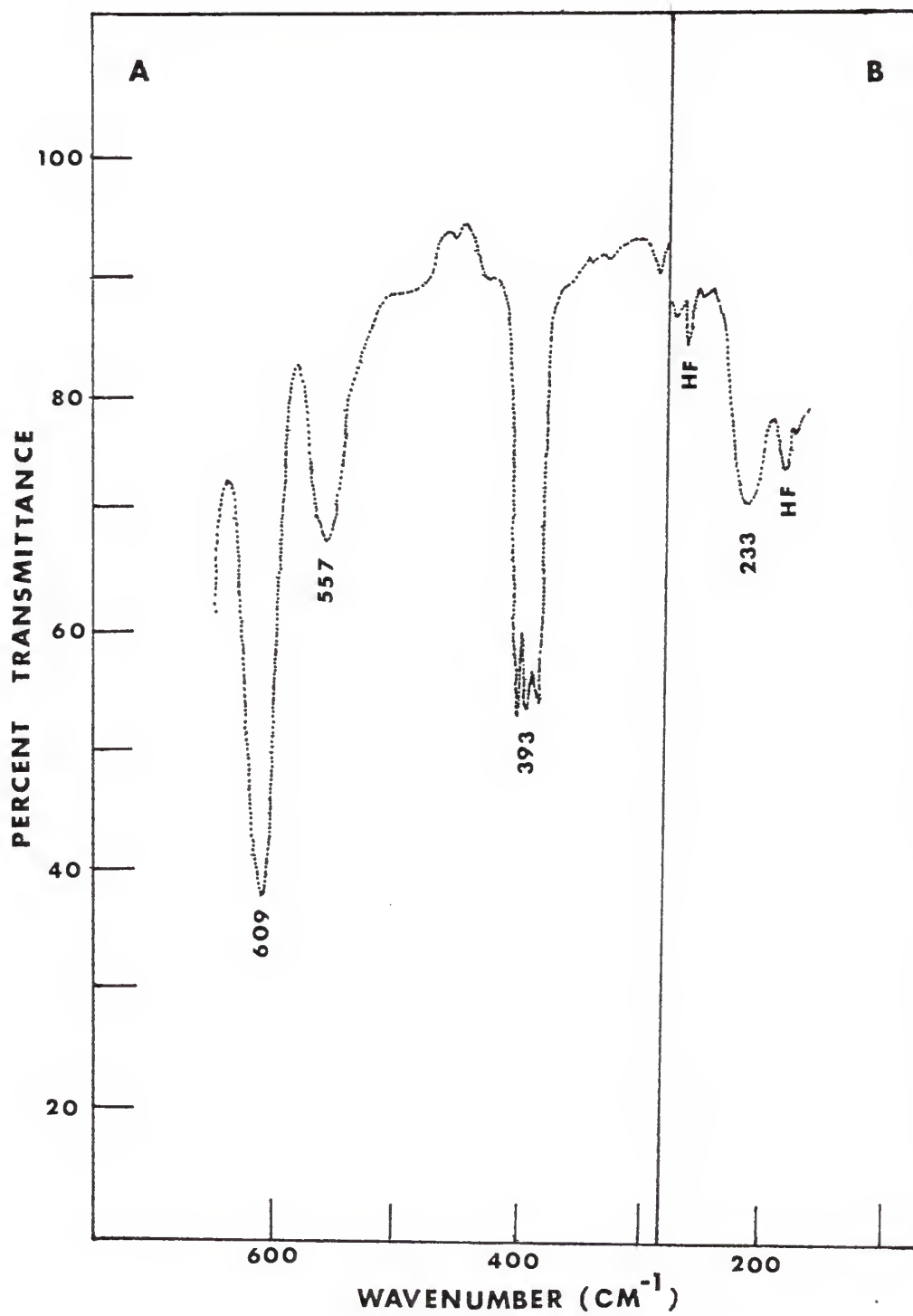
Temperature: $25^{o}C$

EXPLANATION OF FIGURE 7

Raman Spectrum of Liquid CF_3OCl

Spectrometer: JASCO Model R-300

Slit Setting: 150 μm

Sensitivity: 3

Response: 0.5 Seconds

Scan Rate: 4

Source: Ar^+ Laser at 5145 Å

Power: 120 mW

Temperature: -196°C
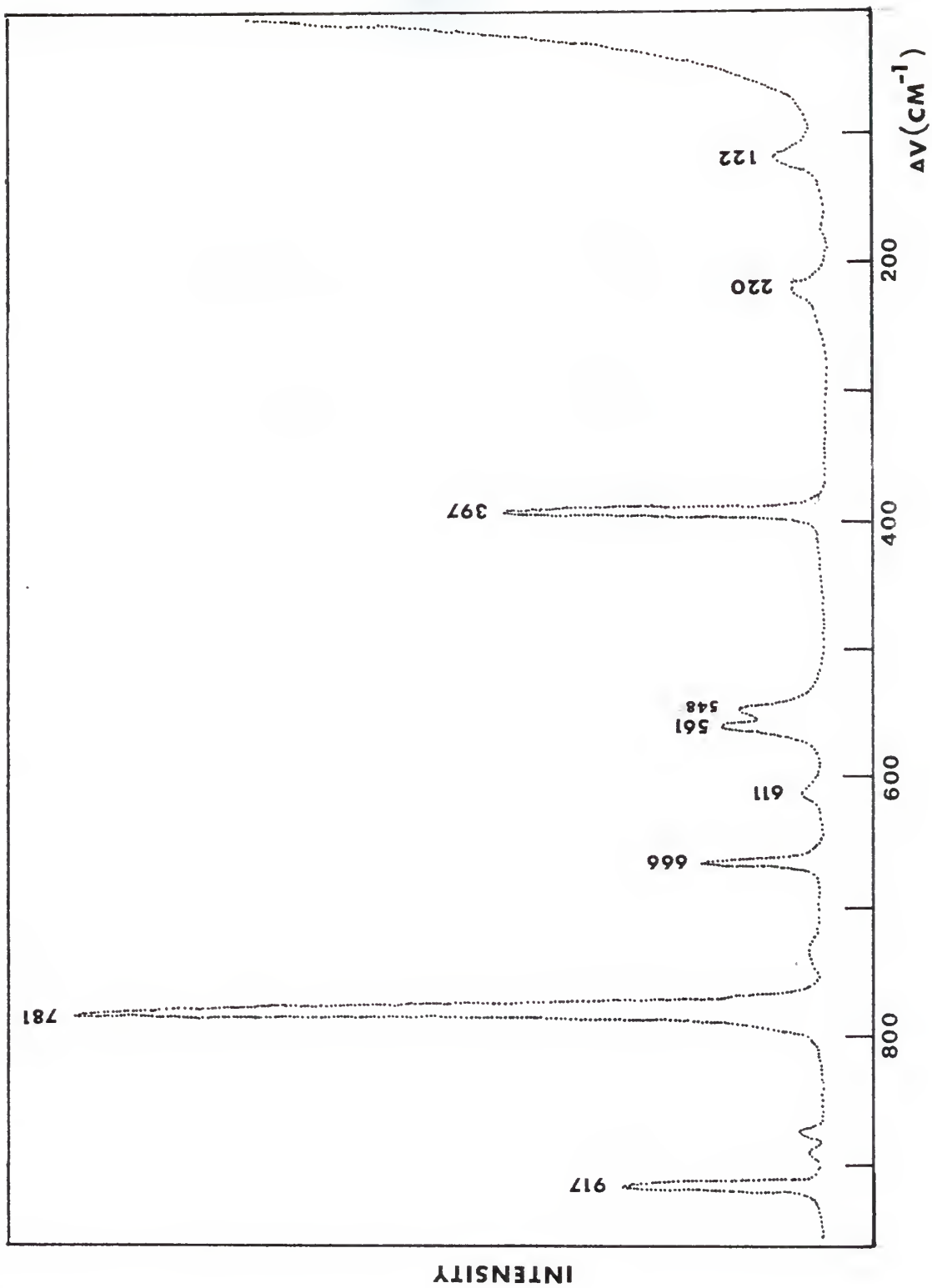
EXPLANATION OF FIGURE 8

High Sensitivity Raman Spectra   of Liquid CF_3OCl

Spectrometer: JASCO Model R-300

Slit Setting: 150 μm

Sensitivity: 5

Response: 2 Seconds

Scan Rate: 4

Source: Ar^+ Laser at 5145 $\overset{o}{A}$

Power: 240 mW

Temperature: $-196^{o}C$
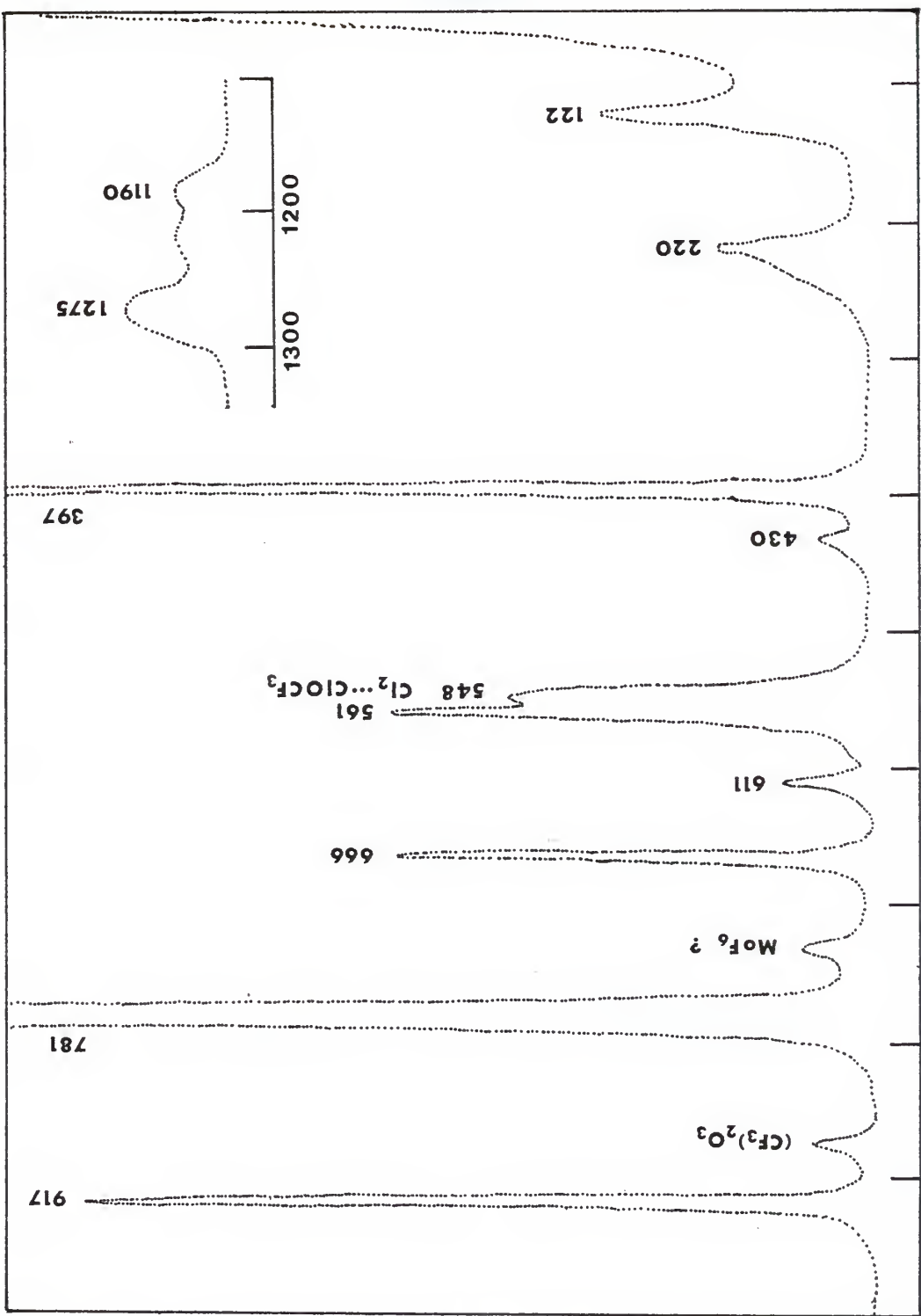
EXPLANATION OF FIGURE 9

ν(OX) and ν(CO) Stretches for CF_3OX Molecules.
(Taken from Reference 5)

A. Figure A. Argon matrix Raman and infrared
    spectra of CF_3OX(X=F,Cl) in the ν(OX) and
    ν(CO) fundamental region. (a) Ar/CF_3OF=100,
    (b) Ar/CF_3OCl=100. Raman spectra were run
    with 5145 Å excitation (1.7 W), 400 CPS
    amplification, 5 cm^{-1} resolution, 0.25 cm/sec
    scan speed and 5 sec time constant.

B. Figure B. Chlorine isotopic splitting of the
    782.7 cm^{-1} Raman band of CF_3OCl in an argon
    matrix at 8°K. Ar/CF_3OCl=100, 5145 Å excit-
    ation (1.7 W), 100 CPS amplification, 4 cm^{-1}
    resolution, 0.05 cm/sec scan speed, 10 sec
    time constant.
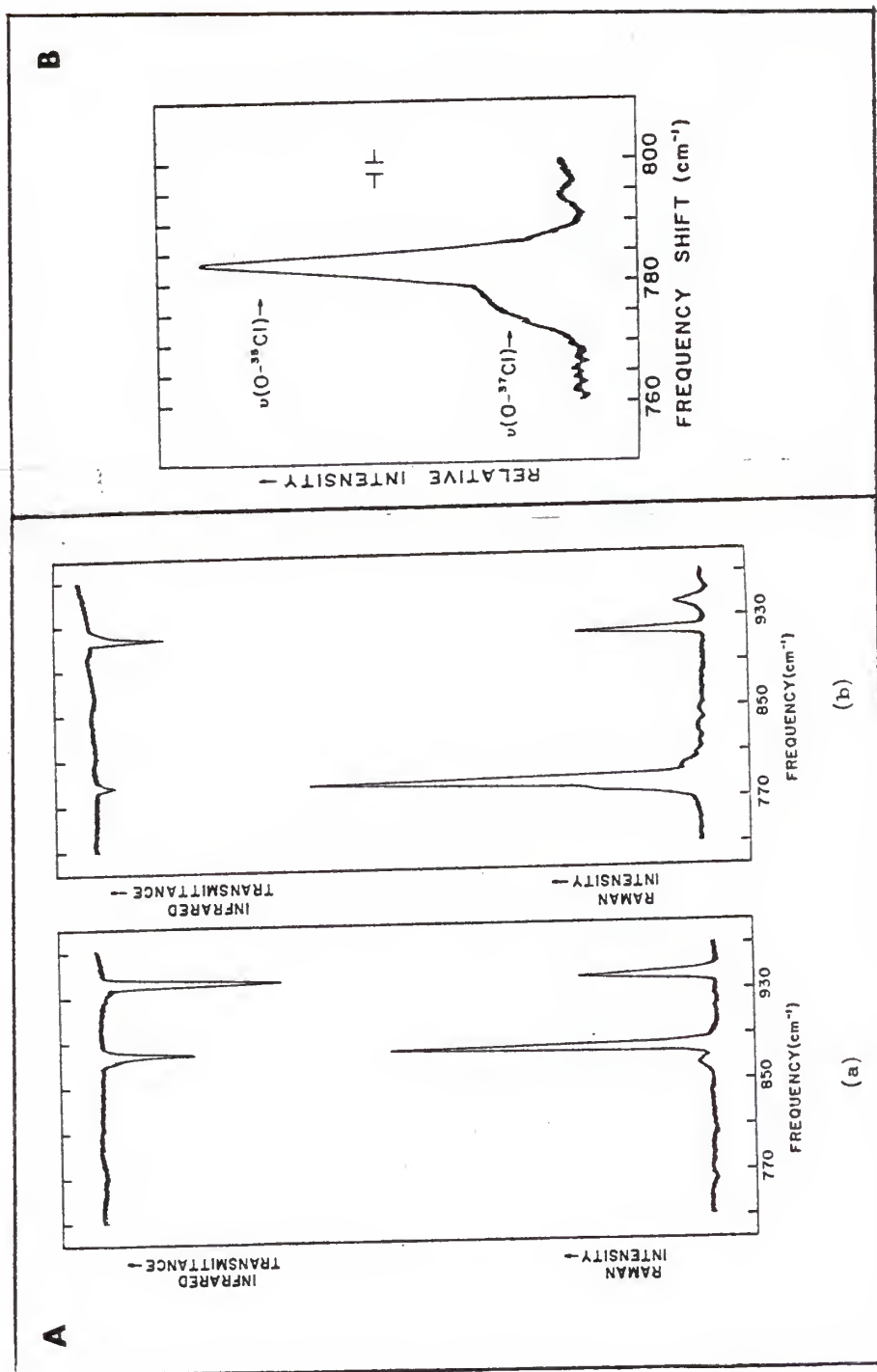
CHAPTER IV
NORMAL COORDINATE ANALYSIS

Having completed the vibrational assignment for the CF_3OX series, it is now possible to carry out a normal coordinate analysis. The purpose of this calculation is to see whether or not the vibrational frequencies chosen as fundamentals in the new assignments can be fitted reasonably well with a realistic potential function. If so, this may be interpreted as evidence for the correctness of the assignment. A second purpose is to clarify the descriptions of the motion in each vibrational mode. A large anount of mixing and very complicated normal coordinates are expected due to the closeness of the masses of atoms in these two molecules.

A. Structural Models

CF_3OF has been shown in a recent electron diffraction study to possess C_s symmetry (13). The geometric parameters of CF_3OF used in this work are listed in Table 3.

Unfortunately no electron diffraction or microwave data for CF_3OCl have been published. Thus, it is necessary to assume bond lengths and interbond angles. CF_3OCl is assumed to be of C_s symmetry with the CF_3O portion of the same geometry as that of CF_3OF. The O-Cl bond related geometry for CF_3OCl is deduced by comparison of CF_3OF with F_2O and F_2O with Cl_2O. Since the O-F bonds in CF_3OF and F_2O differ by only about

0.01 Å, the O-Cl bond length from Cl_2O is used for CF_3OCl. Since the Cl-O-Cl angle in Cl_2O is $8°$ larger than the F-O-F angle in F_2O, the C-O-Cl angle in CF_3OCl is taken as $8°$ larger than the C-O-F angle in CF_3OF. The geometric parameters of CF_3OCl are also shown in Table 3, and the structure of CF_3OX is shown in Figure 10.

B. Construction of the G Matrix

In order to construct the G matices, it is necessary to know the structures of the molecules, the atomic masses, and a set of internal coordinates.

The G matrices used in this study were computed using the programs CART and GMAT which were described in Chapter II. Geometry used for CF_3OF was determined from electron diffraction. Estimated geometry was used for CF_3OCl. These structural parameters are all listed in Table 3 in the previous section. The atomic masses were taken from the carbon 12 system:

$$C(12) = 12.00000$$
$$F(19) = 18.99840$$
$$O(16) = 15.99491$$
$$Cl(35) = 34.96885$$

The G matrix elements were not weighted. Symmetrizations were accomplished using symmetry coordinates shown in Table 4. The internal coordinates used to generate these symmetry coordinates are shown in Figure 11.

Table 3. Structural Data for CF_3OX Compounds

Geometrical Parameters[a]	CF_3OF[b]	CF_3OCl[c]
$R(C-F)(\text{Å})$	1.319	1.319
$R(C-O)(\text{Å})$	1.395	1.395
$R(O-X)(\text{Å})$	1.421	1.700
$\alpha(deg)$	109.4	109.4
$\beta(deg)$	4.1	4.1
$\gamma(deg)$	104.8	112.8
$\delta(deg)$	70.5	70.5
$\theta(deg)$	105.4	105.4
$I_a(\text{amu-Å}^2)$	89.6	89.6
$I_b(\text{amu-Å}^2)$	164.6	254.9
$I_c(\text{amu-Å}^2)$	166.0	256.4
κ	-0.98	-0.99

a. The angles α, β, γ, δ, and θ are illustrated in Figure 10. The asymmetry parameter, κ, is defined as $\kappa = (2B-A-C)/(A-C)$ where A, B, C are rotional constants proportional to $(I_a)^{-1}$, $(I_b)^{-1}$, $(I_c)^{-1}$, respectively. A κ value of -1 corresponds to a prolate symmetric top.

b. The geometry for CF_3OF was determined from the electron diffraction data of Ref. 13.

c. The geometry for CF_3OCl was estimated as discussed in the text. The data used for Cl_2O and F_2O were from L. E. Sutton, ed. "Tables of Interatomic Distances and Configuration in Molecules and Ions", Special Publication No. 11, The Chemical Society, London (1958) p. M67.

EXPLANATION OF FIGURE 10

Structure of CF_3OX Molecules.

Structural data for both molecules are listed
in Table 3.

The dashed line (-----) indicates the C_3 axis
of the CF_3 group which has local C_{3v} symmetry.
The angle of tilt, β, is in the FCOX plane and
is the angle between the C_3 axis and the C-O
bond. For a positive angle of tilt like the
one shown in this figure the F atom in the
FCOX plane is closer to the O atom than are
the two out of plane F atoms.
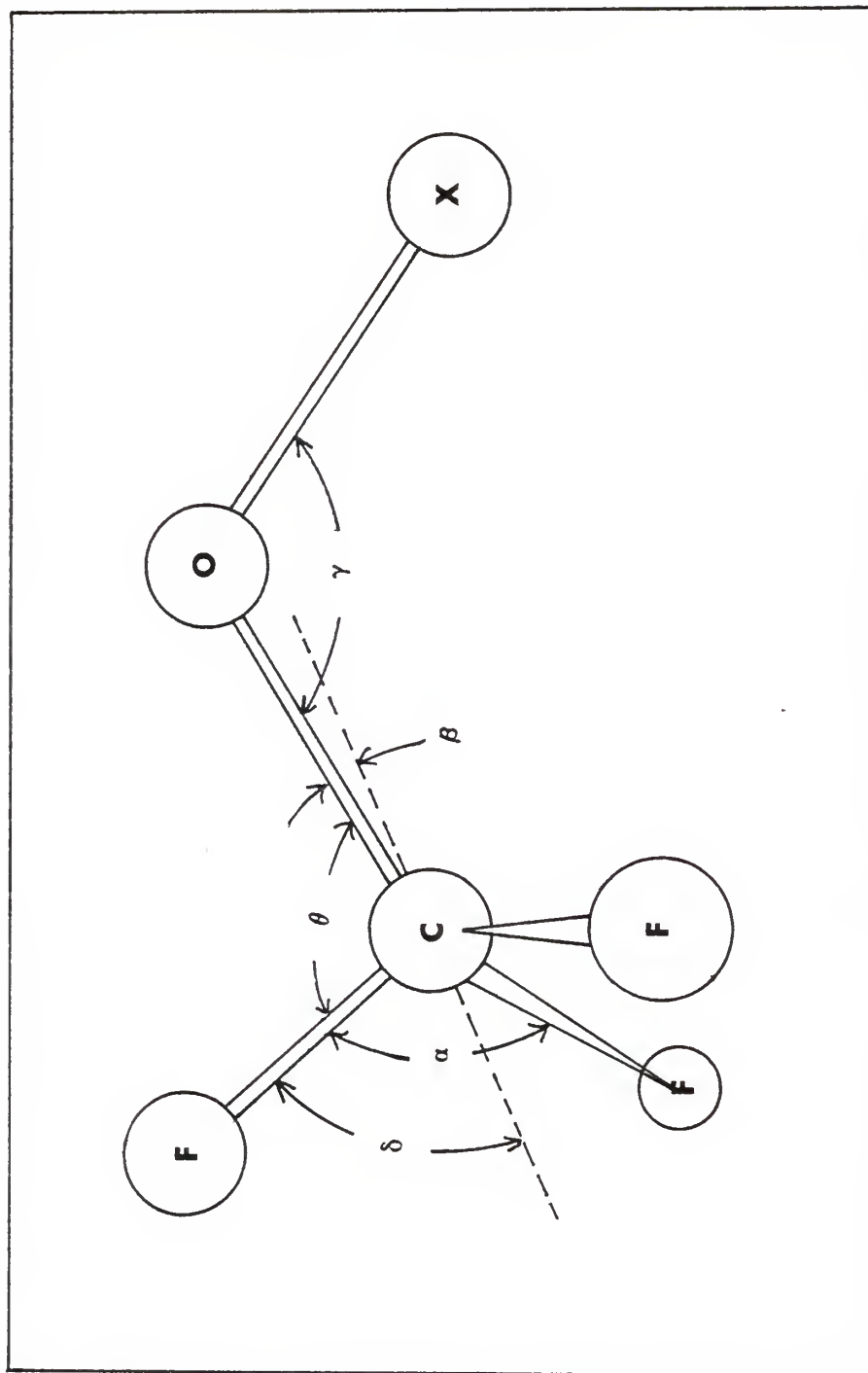
C.   Utilization of Symmetry

Prior to solving the secular equation, the symmetry of the molecular system may be introduced to advantage as a means of simplifying the secular determinant. Symmetry coordinates, which can be constructed from a suitable linear combination of internal coordinates, are used to factor the secular determinant into smaller, square subblocks. The vibrational problem then reduces to the solution of a series of independent, smaller secular determinants.

For the assumed C_s symmetry of the CF_3OX series, group theory analysis (21) predicts twelve normal modes of vibration, eight of species A' (symmetric with respect to the plane of symmetry) and four of species A"(antisymmetric with respect to the plane of symmetry). All twelve are infrared and Raman active, with the A' modes being polarized and A" modes depolarized in the Raman spectrum (4). The symmetry coordinates used to factor the F and G matrices are given in Table 4 in terms of the internal coordinates shown in Figure 11.

D. Choice of Force Fields

The number of vibrational frequencies for a single polyatomic molecule is invariably less than the number of force constants in the general harmonic force field. It was obviously impossible to determine any more than a very limited force field for the CF_3OX series because of the

paucity of data. Since certain interaction constants cannot be determined with any degree of certainty even with a large amount of data (22), we can assume a simplified force field such as the valence force field with selected interaction constants set equal to zero.

The F matrix used in this study was set up in terms of internal coordinates and listed in array form in Figure 12. Symmetrization was obtained by using the symmetry coordinates listed in Table 4. The least squares adjustment of force constants were carried out using the program FPERT described earlies.

Results of the force constant analysis for CF_3OF and CF_3OCl are shown in Tables 5, 6, and 7. The meaning of 'Chemical Fitting' and 'Mathematical Fitting' appearing in Tables 6 and 7 will be explained in the next section.

E.   Chemical Approach vs. Mathematical Approach

A complete and reliable specification of the potential energy of a molecular system serves as the primary goal of a normal coordinate analysis. The most common approach toward evaluating a potential function from observed vibrational frequencies involves some method of force constant adjustment such that the calculation reproduces the observed data as closely as possible (22-26). In most cases, harmonic frequencies are not available and consequently anharmonicity effects are an additional source of error. We are using

experimental frequencies not harmonic frequencies in this work.

The method of least-squares fitting, which was employed in this study, represents a particularly effective procedure for refining an initial set of force constants to optimize the fit between the calculated and observed frequencies. This mathematical approach, as we may put it, regards the vibrational analysis as a problem in applied mathematics and there is no relationship between force constant values and chemistry. Since the method for adjusting force constants does not insure a unique potential function, other molecular information may be used as constraints in limiting the acceptable solutions of the secular equation(1).

The imposed constraints represent a kind of chemical approach. In this approach the chemistry of this molecule should be taken into consideration. The force constants must be consistent with other data about the compound, including the known chemical properties of this compound and with a related series of compounds it should be possible to transfer force constants for similar group. Although the transfer-ability of force constants is not always expected to be strictly observed, it should be consistent within certain ranges obtained from similar molecules.

Without proper choice and restraint on the major diagonal force constants, the mathematical fitting minimum found by

least-squares analysis may be just another incorrect minimum on the fit $\underline{vs}$. force constant set surface. The fitting may be greatly improved with no restriction on major diagonal force constants. The final mathematical fitting solution certainly need not correspond to the real molecule and this solution may not have any chemical significance.

From our work the difference of these two approaches is very clear in the case of CF_3OCl. The mathematical fitting is excellent, but the force constant for OCl stretching must be raised to an unreasonably high value to get this excellent fit. All the discussion in the next chapter is based entirely on the results of chemical fitting.

Table 4.   Symmetry Coordinates for CF_3OX Molecules
of C_s Symmetry[a]

	Antisymmetric CF_3 stretch	$S_1 = \sqrt{6}^{-1}(2\Delta r_4 - \Delta r_5 - \Delta r_6)$
	Symmetric CF_3 stretch	$S_2 = \sqrt{3}^{-1}(\Delta r_4 + \Delta r_5 + \Delta r_6)$
	OX stretch	$S_3 = \Delta d$
	Antisymmetric CF_3 deformation	$S_4 = \sqrt{6}^{-1}(2\Delta \alpha_4 - \Delta \alpha_5 - \Delta \alpha_6)$
A'	Symmetric CF_3 deformation	$S_5 = \sqrt{6}^{-1}(\Delta \alpha_4 + \Delta \alpha_5 + \Delta \alpha_6 - \Delta \beta_4 - \Delta \beta_5 - \Delta \beta_6)$
	COX bend	$S_6 = \Delta \gamma$
	CO stretch	$S_7 = \Delta l$
	CF_3 rock (in-plane)	$S_8 = \sqrt{6}^{-1}(2\Delta \beta_4 - \Delta \beta_5 - \Delta \beta_6)$
	Redundant	$S_9^b = \sqrt{6}^{-1}(\Delta \alpha_4 + \Delta \alpha_5 + \Delta \alpha_6 + \Delta \beta_4 + \Delta \beta_5 + \Delta \beta_6)$
	Antisymmetric CF_3 stretch	$S_{10} = \sqrt{2}^{-1}(\Delta r_5 - \Delta r_6)$
	Antisymmetric CF_3 deformation	$S_{11} = \sqrt{2}^{-1}(\Delta \alpha_5 - \Delta \alpha_6)$
A''	CF$_3$ rock (out-of-plane)	$S_{12} = \sqrt{2}^{-1}(\Delta \beta_5 - \Delta \beta_6)$
	CF_3 torsion	$S_{13} = \Delta \tau$

a.   There will be three related quantities having numbering
systems as follows: these thirteen symmetry coordinates,
S_i, (including one redundancy in the A' symmetry block),
twelve cooresponding normal coordinates, Q_i, in Tables
10 and 11, and twelve normal mode frequencies, v_i, in
Tables 6, 7, 9, 12, 13, and 14. The relation between the
three numbering systems is given in Table 6.

b.   These coordinates are correct for tetrahedral C_{3v} angles.
However, they may be used for the non-tetrahedral angle
case since the redundancy is removed during diagonali-
zation of the G matrix.

EXPLANATION OF FIGURE 11

Internal Coordintes for CF_3OX Molecules.

C_s symmetry is assumed with the F, C, O,
and X atoms in the same plane.
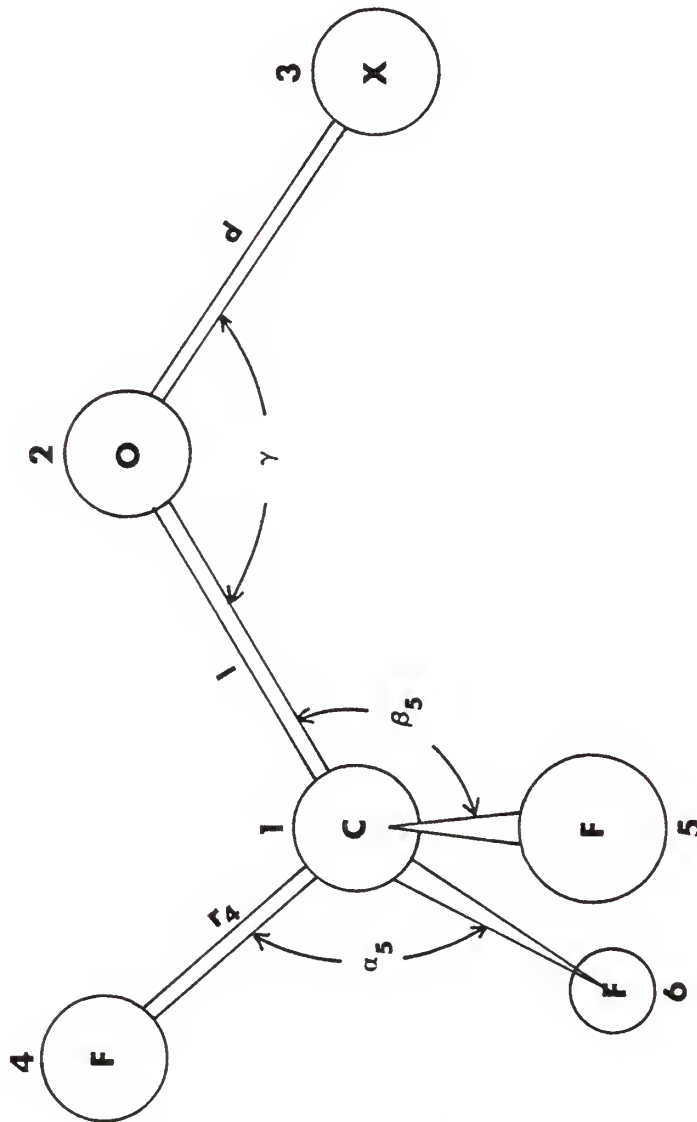
EXPLANATION OF FIGURE 12

Unsymmetrized F Matrix for CF_3OX Molecules.
Internal coordinates are from Figure 11. The
F matrix elements $r\alpha$ and $\alpha\beta$ are for three
opposite pairs of internal coordinates. The F
matrix elements $r\alpha'$ and $\alpha\beta'$ are for six adjacent
pairs of internal coordinates. The F matrix
elements $r\beta$ are for three adjacent pairs of
internal coordinates. The F matrix elements $r\beta'$
are for six opposite pairs of internal coordinates.

		1	2	3	4	5	6	7	8	9	10	11	12	13
		r_4	r_5	r_6	l	d	α_4	α_5	α_6	β_4	β_5	β_6	γ	τ
1	r_4	r	rr	rr	rl	o	rα	rα'	rα'	rβ	rβ'	rβ'	o	
2	r_5		r	rr	rl	o	rα'	rα	rα'	rβ'	rβ	rβ'	o	
3	r_6			r	rl	o	rα'	rα'	rα	rβ'	rβ'	rβ	o	
4	l				l	ld	lα	lα	lα	lβ	lβ	lβ	lγ	
5	d					d	o	o	o	o	o	o	dr	
6	α_4						α	αα	αα	αβ	αβ'	αβ'	o	
7	α_5							α	αα	αβ'	αβ	αβ'	o	
8	α_6								α	αβ'	αβ'	αβ	o	
9	β_4									β	ββ	ββ	o	
10	β_5										β	ββ	o	
11	β_6											β	o	
12	γ												γ	
13	τ													τ

Table 5. Internal Coordinate Force Constants[a,b] for CF_3OF and CF_3OCl

Internal Force Constant[c]	CF_3OF Chemical Fitting	CF_3OF Mathematical Fitting	CF_3OCl Chemical Fitting	CF_3OCl Mathematical Fitting
r	6.950	6.775	6.950	6.846
l	5.200	5.656	5.200	5.877
d	3.850±0.220	3.785±0.035	2.800±0.556	3.885±0.063
α	2.000	1.980	2.050	1.836
β	1.200	1.235	1.150	1.266
γ	1.800±0.172	1.918±0.027	1.700±0.377	2.014±0.042
τ	0.0167±0.0001	0.0165±0.0001	0.0161±0.0019	0.0165±0.0002
r r	0.900	1.120	0.900	0.734
r l	0.850	0.850	0.900	0.850
l d	1.000±0.243	0.425±0.095	0.300±1.294	0.896±0.199
r α(opp.)	0.120	0.120	0.120	0.120
r α'(adj.)	0.910	0.950	0.910	1.040
r β(adj.)	0.750	0.500	0.700	0.775
r β'(opp.)	0.100	0.100	0.100	0.100
l α	0.200	0.200	0.200	0.200
l β	0.600	0.600	0.600	0.600
l γ	0.000±0.245	0.614±0.055	0.100±0.933	0.816±0.113
d γ	0.250±0.200	0.456±0.027	0.100±0.333	0.918±0.041

Internal Force Constant[c]	CF_3OF Chemical Fitting	CF_3OF Mathematical Fitting	CF_3OCl Chemical Fitting	CF_3OCl Mathematical Fitting
$\alpha\alpha$	0.300	0.300	0.350	0.300
$\alpha\beta$(opp.)	0.000	0.000	0.000	0.000
$\alpha\beta'$(adj.)	0.150	0.150	0.150	0.150
$\beta\beta$	0.100	0.100	0.100	0.100

a. Stretching constants in units of millidynes per angstrom. Stretch-bend interaction constants in units of millidynes per radian. Bending and torsion constants in units of millidyne angstrom per square radian.

b. The force constants $\mathbf{d}$, γ, τ, $\mathbf{ld}$, $\mathbf{l\gamma}$, and $\mathbf{d\gamma}$ associated with the OX part of the CF_3OX structure are likely to change from CF_3OF to CF_3OCl and are of primary concern. The remaining force constants have been transfered or estimated using GF_4 (53) and GF_3H (54). Error estimates corresponding to a set of force constants can be obtained for a restricted number of members of the set by using the set as input to the FPERT program with the re-stricted number of members of the set allowed to vary and with the number of perturbations restricted to zero. The errors shown for d, γ, τ, ld, lγ and dγ are obtained this way and are the errors listed as * in the FPERT output and calculated using λ_i(obs) - λ_i(calc) where $\lambda = 4\pi^2 c^2 \nu^2$ (see numbered statement 62 in the FINI subroutine of FPERT in Tech. Report No. 57-65 in. reference 10).

c. See Figures 11 and 12 for definition of these internal coordinates.

Table 6. Assignments of the Fundamental Vibrations[a]
of Trifluoromethyl hypofluorite (CF_3OF)

ν_i	Approximate description	Obs[b]	Chemical Fitting	Mathematical Fitting
	A' Species			
1	Antisym CF_3 stretch	1294	1321	1299
2	Sym CF_3 stretch	1222	1214	1222
3	CO stretch	947	941	948
4	OF stretch	882	883	882
5	Sym CF_3 deformation	678	674	678
6	Antisym CF_3 deformation	585	589	585
7	COF bend	429	420	429
8	In-plane CF_3 rock	278	267	278
	A" Species			
9	Antisym CF_3 stretch	1261	1256	1251
10	Antisym CF_3 deformation	607	616	608
11	Out-of-plane CF_3 rock	431	429	431
12	CF_3 torsion	127	128	127
	Average error		1.15%	0.137%

a. The numbering system for the normal mode frequencies,
ν_i, normal coordinates, Q_i, and symmetry coordinate,
S_i, are related as follows:

ν_i 1 2 3 4 5 6 7 8 - 9 10 11 12
Q_i 1 2 3 4 5 6 7 8 - 9 10 11 12
S_i 1 2 7 3 5 4 6 8 9 10 11 12 13

As shown in Table 4, S_9 is the redundant symmetry coordinate
in the A' symmetry block.

b. Frequencies are from gas phase infrared spectra (Table 1)
except the CF_3 torsion is from gas phase Raman spectra
(5, 19).

17
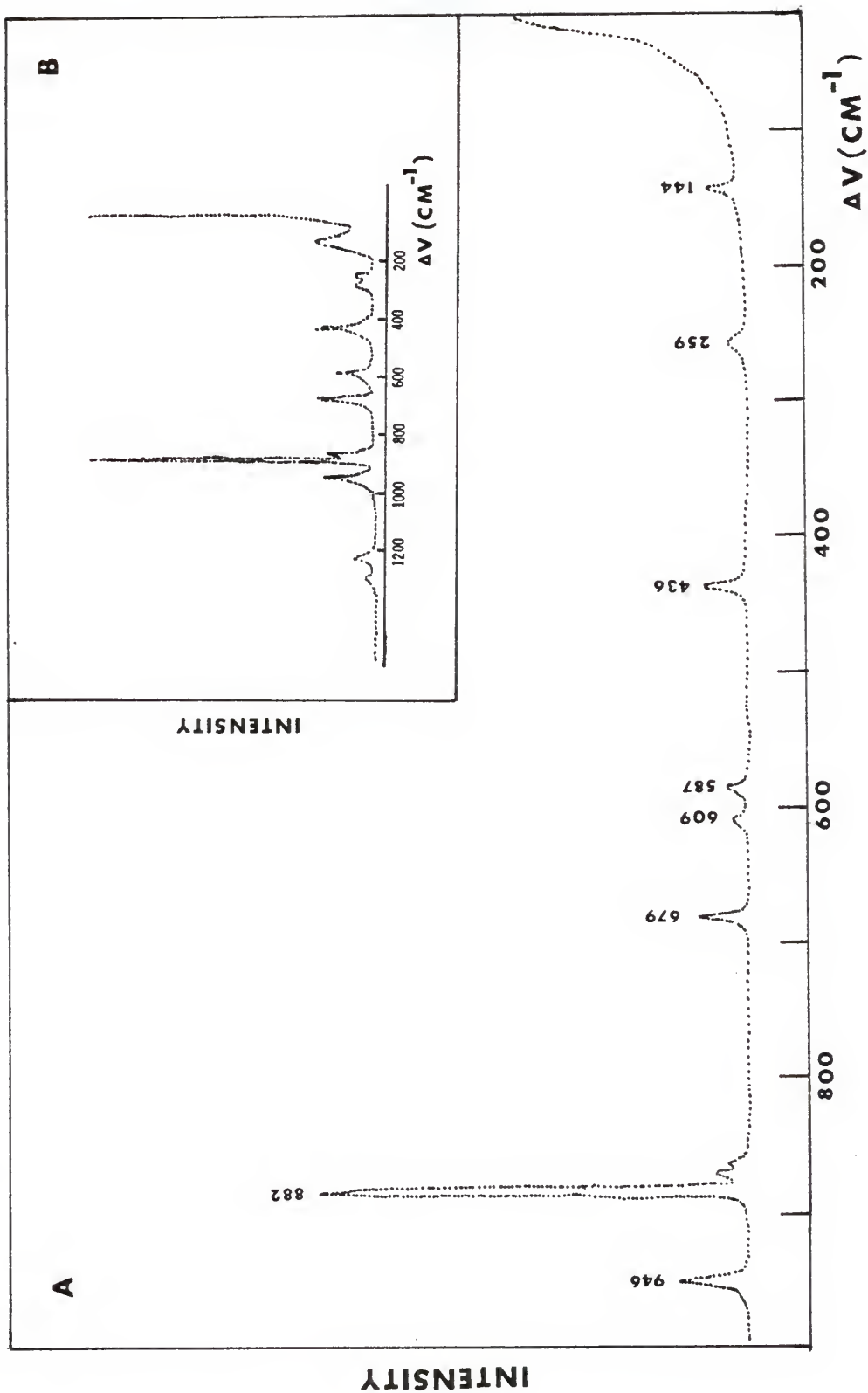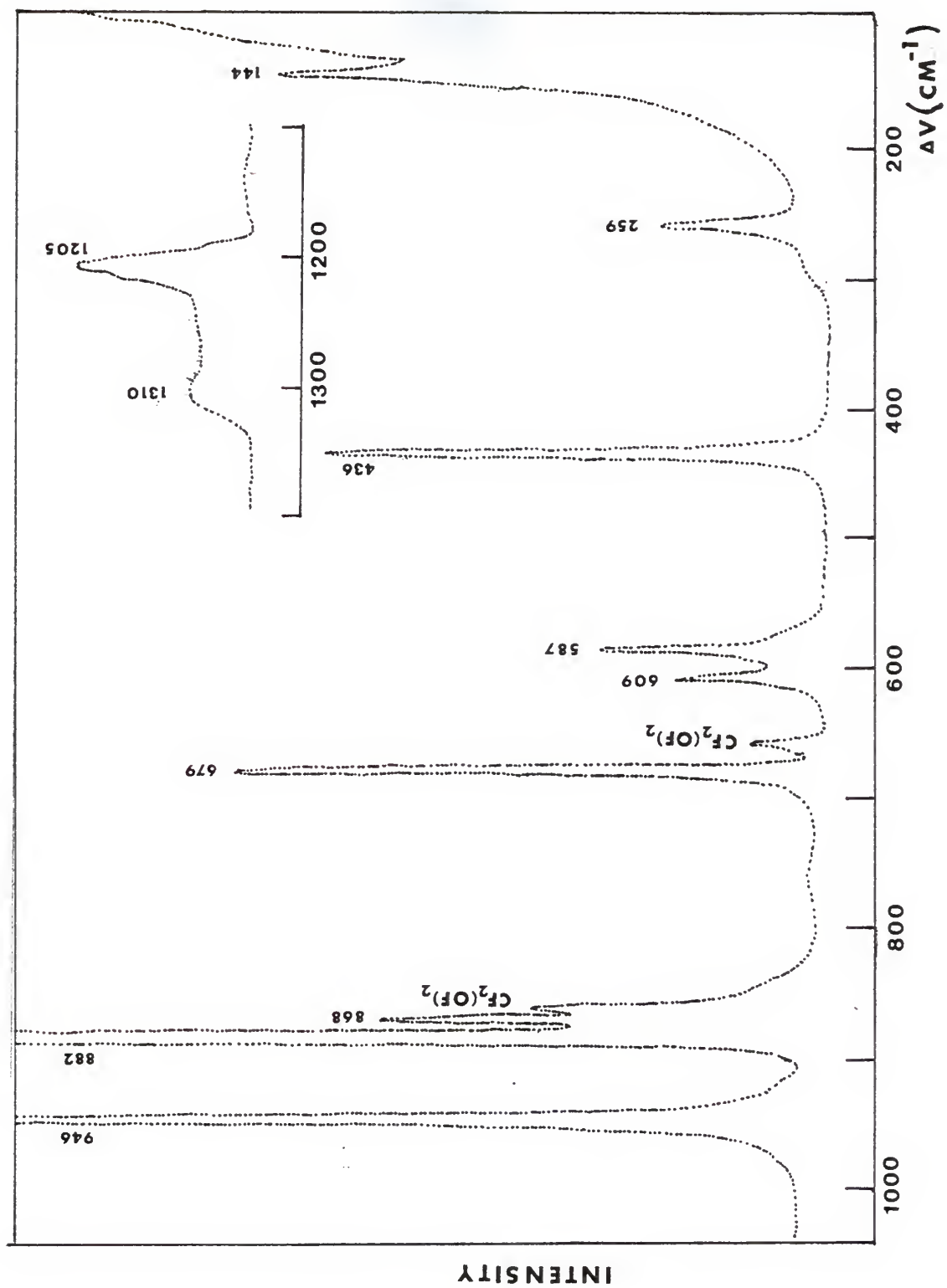
Table 2. Raman and Infrared Data for CF$_3$OCl below 1400 cm^{-1}

Gas IR[a]	Liquid Raman[a]	ρ[b]	Ar Matrix Raman[c]	Assignments[d]
1271	1275	0.60	1269	a.ν_{CF_3}(A')
1230			1221	a.ν_{CF_3}(A")
1213	1190	0.66	1200	s.ν_{CF_3}
919(Q)[e]	917	0.46	920	ν_{CO}
780	781	0.12	783	ν_{OCl}35
			776	ν_{OCl}37
665(Q)[e]	666	0.38	663	s.δ_{CF_3}
609	611	0.76	609	a.δ_{CF_3}(A")
557	561	0.26	558	a.δ_{CF_3}(A')
	430	?		ρ_{CF_3}(A")
393(Q)[e]	397	0.27	398	δ_{COCl}
233	233?		239	$2\tau_{CF_3}$ and
220??	220	0.47		ρ_{CF_3}(A')
-	122	0.81		τ_{CF_3}

a. D. D. DesMarteau and R. M. Hammaker, unpublished studies.

b. These depolarization ratios for the liquids were measured by rotating the polarization of the incident laser beam with no analyzer and no scrambler in the scattered beam Known depolarized bands below 500 cm^{-1} gave depolarization ratios between 0.75 and 0.89 with this arrangement. The arrangement is method IV in H. H. Claassen, H. Selig, and J. Shamir, Appl. Spectroscopy, 23, 8 (1969).

c. References (5) and (19).

d. These symbols refer to the word description of the symmetry coordinates defined in Table 4 and of the fundamental vibrations in Table 6.

e. These are Q branches for bands having PQR structure as follows: 915, 919, 923; 659, 665, 671; 386, 393, 399.

Table 7. Assignments of the Fundamental Vibrations[a]
of Trifluoromethyl Hypochlorite (CF_3OCl)

ν_i	Approximate Description	Obs[b]	Chemical Fitting	Mathematical Fitting
		A' Species		
1	Antisym CF_3 stretch	1271	1309	1273
2	Sym CF_3 stretch	1213	1208	1213
3	CO stretch	919	935	919
4	OCl stretch	780	774	783
5	Sym CF_3 deformation	665	658	664
6	Antisym CF_3 deformation	557	571	558
7	COCl bend	393	348	392
8	In-plane CF_3 rock	233	217	233
		A" Species		
9	Antisym CF_3 stretch	1230	1262	1229
10	Antisym CF_3 deformation	609	613	608
11	Out-of-plane CF_3 rock	430	422	430
12	CF_3 torsion	108	108	110
Average error			2.72%	0.265%

a. See footnote a in Table 6.

b. Frequencies are from gas phase infrared spectra (Table 2)
with the following exceptions: 430 cm^{-1} from liquid
Raman and 108 cm^{-1} estimated as liquid Raman less 11.8%
(122 cm^{-1} - 14 cm^{-1} = 108 cm^{-1}) since CF_3OF has gas
phase Raman frequency 11.8% below liquid Raman frequency
for the CF_3 torsion. See footnotes a and b in Table 9.

CHAPTER V

RESULTS, CONCLUSION, AND OTHER REMARKS

Results of the force constant analyses of CF_3OF and
CF_3OCl are shown in Tables 5, 6 and 7.

Numerical values of the force constants are reproduced
in Table 5 whereas the calculated fundamental frequencies
are compared with the observed values in Tables 6 and 7.

A. Comments on the Choice of Force Fields

It can be seen that the agreement of calculated and
observed frequencies for the twelve fundamental modes is
'good' for chemical fitting but 'excellent' for mathematical
fitting. If the correctness of force field is measured by
the accuracy of the frequency fit, it is very obvious what
the choice should be.

But for a case like ours where CF_3OF, CF_3OCl, $CF_3OOH(D)$,
CF_3OOF, and CF_3OOCl all have a CF_3O fragment in common, the
explicit recognition of the importance of chemical factors
become increasingly pertinent to normal coordinate analysis
and will be the criterion of a reasonable force field.

CF_3OF is thermally stable in the IR cell at room tem-
perature and the gas phase Raman spectra can be obtained at
room temperature with Ar^+ laser radiation. CF_3OCl is stable
at room temperature only under scrupulously dry, inert
condition. Photolytic decomposition of CF_3OCl is quite rapid
and the decomposition products found are consistent with a

two-step reaction path involving the two radicals $CF_3\cdot$ and $Cl\cdot$ (3). In the course of this work, the CF_3OCl began to decompose during the recording of its IR spectrum at ambient temperature. Smardzewski and Fox (5) reported that CF_3OCl photolyzed almost immediately upon trying to record its gas phase Raman spectrum at room temperature with an Ar^+ laser.

This evidence suggests that the O-F bond in CF_3OF may be stronger than the O-Cl bond in CF_3OCl. Chemical consideration would prohibit the use of about the same values for the force constants of the O-X bond. Then identical or very similar values for the force constants related to the CF_3O fragment should be observed while the O-X bond related force constants should be allow to vary in CF_3OF and CF_3OCl independently to improve the fit in both molecules.

Pierce, Di Cianni, and Jackson (27) as well as Morino and Saito (28) have done a good analysis on F_2O and the OF stretching force constant $d(OF)$ was determined to be 3.78 or 3.95 or 4.10 mdyn/Å by several methods.

The $d(OF)$ values in HOF obtained by Noble and Pimentel (29) and Ogilvie (30) are 4.37 and 4.27 mdyn/Å, respectively. Noble and Pimentel have suggested that $d(OF)$ is larger in HOF that in F_2O because the electronegativity of fluorine weakens the O-H bond and strengthens the O-F bond by attraction of negative charge out of the O-H bond into the O-F bond. For such a charge competition in CF_3OF, it seems reasonable that

the CF_3 group would be better able to compete with the F atom for charge over the CF_3OF frame. Thus d(OF) in CF_3OF should be smaller than that in HOF. The value of 3.85 mdyn/Å used in this study can be considered to be a chemically re-sonable value, since it is in the range for F_2O.

Rochkind and Pimentel(31) should have the most reliable force field for Cl_2O in view of their isotopic data. The low value of 2.75 mdyn/Å for d(OCl) in Cl_2O is commensurate with the relatively long Cl-O bond of 1.70 Å. This value was proclaimed to be the prototype force constant for a normal Cl-O single bond (31). Repetition of the calculation on Cl_2O gave d(OCl) the values of 2.75(32) and 2.88(33) mdyn/Å respectively. A value of 2.65 mdyn/Å was obtained for d(OCl) in $ClO_3OCl(34)$. The work of Witt and Hammaker(35) on the skeletal mode of Cl_2O_7 put a value of 3.09 mdyn/Å on the skeletal OCl stretch.

Bond-stretching force constants, d(OF) and d(OCl), taken from related molecules containing O-F and O-Cl bonds are listed in Table 8 for comparison.

The electronegativity arguments of Noble and Pimentel can be applied to the d(OCl) value in HOCl and CF_3OCl also. Certainly, the chlorine is electronegative enough relative to hydrogen to attract charge out of the O-H bond into the Cl-O bond. Thus d(OCl) in HOCl should be larger than in Cl_2O. One might argue that replacement of H by CF_3 would shift

some charge away from the Cl-O bond into the C-O bond as
the CF_3 group would be better able to compete with Cl for
charge over the C-O-Cl frame than would H over the HOCl
frame. Thus d(OCl) in CF_3OCl should be smaller than in HOCl.

From Table 8 we can observe that the previous work is
generally consistent with d(OF) larger than d(OCl) with the
difference ranging from 0.6 to 1.2 mdyn/Å. Judging from the
above argument, we believe the values of d(OX) of CF_3OX
should close to those of X_2O. The force field with d(OCl)
higher than or close to d(OF) should be dismissed.

Table 8.   Bond-stretching Force Constants of O-F
and O-Cl Bonds from related Molecules

| Compound | Force Constants | |
	d(OF)(mdyn/Å)	d(OCl)(mdyn/Å)
F_2O[a]	3.95	
Cl_2O[b]		2.75
ClO_3OF[c]	3.56	
ClO_3OCl[c]		2.65
HOF[d]	4.27	
$HOCl$[d]		3.68

a.   Data from Ref. 27.
b.   Data from Ref. 31.
c.   Data from Ref. 35.
d.   Data from Ref. 30.

B. Comments on Assignments Implied by Force Conatant Calculation

Three fundamentals are expected in the region between 1180 and 1300 cm^{-1} for the CF_3 stretching modes (ν_{CF_3}) of the CF_3OX series. Two of species A' and one of species A" are expected under C_s symmetry. Our calculations gave a better fit for ν_{CF_3} if the highest and lowest frequencies are in the A' block and middle frequency is in the A" block. This indicates that the assignments of the middle frequency (1261 cm^{-1}) in the A' block and lowest frequency (1222 cm^{-1}) in the A" block for antisymmetric CF_3 stretching by Wilt and Jones (4) should be reversed. This sequence is used in final assignments of six compounds in both the CF_3OX and CF_3OOX series (8).

Initially our sample of CF_3OF showed many Raman bands in addition to those in Figures 3 and 4. These were shown to be due to $CF_2(OF)_2$. In the preparation of CF_3OF by addition of F_2 to COF_2, CO_2 impurity in the COF_2 can add two moles of F_2 to form $CF_2(OF)_2$. The sample of CF_3OF in Figures 3 and 4 has had most of the $CF_2(OF)_2$ separated by low temperature chromatography and only two small peaks remain corresponding to strong bands from $CF_2(OF)_2$. Following this purification, a band at 868 cm^{-1} remained which was not due to $CF_2(OF)_2$. Smardzewski and Fox (5,19) report an analogous band for CF_3OF in both the gaseous and Ar matrix Raman spectra. We

assign this band to $2 \delta_{COF}$ in Fermi resonance with ν_{OF}.
Using the method developed by Dixon (36) and used by Saier,
Cousins and Basila (37), we calculate that a Fermi resonance
perturbation of only 1-3 cm^{-1} would be necessary to give
the intensity of the 868 cm^{-1} band relative to the 882 cm^{-1}
band in Figure 3, if the 868 cm^{-1} band had zero intensity in
the absence of Fermi resonance.

Both CF_3OX compounds have two bands in the IR and Raman
spectra between 200 and 300 cm^{-1}. Initially it was assumed
that both were CF_3 rocking modes, ρ_{CF_3}, with the one in the
A' block expected to be stronger in the Raman and the one in
the A" block expected to be stronger in the IR.

The force constant calculations leave little doubt that
the two rocking modes, ρ_{CF_3}, are far apart with the one in
the A" block for CF_3OX under C_s symmetry being in the sur-
prisingly high frequency range 400-500 cm^{-1}.

The microwave result (6) for CF_3OF requires the 0 → 1
assignment in the CF_3 torsion, τ_{CF_3}, to the lowest frequency
in the liquid Raman (144 cm^{-1}) and gas phase Raman (127 cm^{-1})
spectra for CF_3OF and by inference for CF_3OCl and other CF_3OOX
series members also.

The choice of "$2 \tau_{CF_3}$" and "$\rho_{CF_3}(A')$" for the bands
between 200 and 300 cm^{-1} is not unambiguous. If one band is
above 2 x ("τ_{CF_3}"), and the other is slightly below 2 x
("τ_{CF_3}"), then the former is "$\rho_{CF_3}(A')$" and the latter is

"2 τ_{CF_3}". Such a comparison should be made with all frequencies from the same phase since the vapor torsion frequency is 17 cm^{-1} lower than the liquid frequency in the Raman spectra for CF$_3$OF. In general low frequency modes tend to increase in frequency upon condensation in contrast to stretching modes which tend to decrease in frequency upon condensation (38). Considering each phase separately, Table 9 was established to analyze the assignments of these two bands.

The frequency tabulation shown in Table 9 suggests 278 and 233 cm^{-1} as the correct choice for " $\rho_{CF_3}(A')$ " for gaseous CF$_3$OF and CF$_3$OCl, respectively. However, comparison across the " $\rho_{CF_3}(A')$ " row has the gaseous frequencies at higher values than the condensed phase frequencies contrary to normal expectations. It is, of course, possible that the nature of the normal mode could account for the frequencies being higher in the gas. Another disturbing feature is that the 252 cm^{-1} band is more intense than the 278 cm^{-1} band in the gaseous IR spectrum of CF$_3$OF. It is possible that the 278 cm^{-1} band is a part of the contour of a " $\rho_{CF_3}(A')$ " mode between 220 and 300 cm^{-1} with a center near 265 cm^{-1} and superposition of "2 τ_{CF_3}" near 250 cm^{-1} causes an apparent maximum at 252 cm^{-1}. The Raman gas bands (5) of CF$_3$OF at 272 and 246 cm^{-1} are of equal intensity and could be the contour of a single band. In the Raman spectra in an Ar matrix, only one band occurs for both CF$_3$OF and CF$_3$OCl. We assume that

Table 9. Frequency Comparison for Bands in the 200-300 cm^{-1} Region for CF$_3$OX Compounds

	CF$_3$OF				CF$_3$OCl			
	Raman gas	Raman liquid	Raman Ar matrix	IR gas	Raman gas	Raman liquid	Raman Ar matrix	IR gas
ρ_{CF_3} (A')	272	259	256	278	---	220	239	233
2τ_{CF_3} (A')	246	285?	---	252	---	233?	---	220
τ_{CF_3} (A")	127	144	---	(127)[a]	---	122	---	(108)[b]

a. Since we can't observe IR bands below about 160 cm^{-1} on our Perkin-Elmer Model 180 spectrophotometer, we must use gas phase Raman frequencies or calculated values. Using the gas phase Raman data of Ref. 5 and our liquid Raman data for CF$_3$OF as reference, we get an 11.8% frequency shift from Raman liquid frequency to Raman gas frequency for the torsional mode.

b. Applying the same 11.8% frequency shift to CF$_3$OCl Raman liquid data at 122 cm^{-1} we can get the vapor frequency of the torsional mode of CF$_3$OCl at 108 cm^{-1}. This computational process is shown below:

Compound	Raman liquid	Raman gas	Shift	% shift
CF$_3$OF	144 cm^{-1}	127 cm^{-1}	17 cm^{-1}	11.8
CF$_3$OCl	122 cm^{-1}	108 cm^{-1}	14 cm^{-1}	11.8

band is "$\rho_{CF_3}(A')$". However, since the Ar matrix is too
highly scattering to permit close enough approach to the
Rayleigh line to observe "τ_{CF_3}" there is no opportunity to
confirm that the single Raman band is above "$2 \tau_{CF_3}$" and is
most probably "$\rho_{CF_3}(A')$" rather than "$2 \tau_{CF_3}$". Since matrix
shifts from the gas are often only a few cm^{-1}, the single
matrix frequency assumed to be "$\rho_{CF_3}(A')$" matches best
with 252 (or 265) cm^{-1} for the CF_3OF gaseous IR spectrum.

For gaseous CF_3OCl one can justify the use of 233 cm^{-1}
as "$\rho_{CF_3}(A')$" on the grounds that it is more intense than
the 220 cm^{-1} absorption which is a shoulder in the IR of the
gas. Also 233 cm^{-1} is closer to the Ar matrix frequency which
usually approximates gas frequencies more closely than liquid
frequencies, we assume a single band in the Raman spectrum
in the Ar matrix is "$\rho_{CF_3}(A')$".

For CF_3OF the Q branch at 429 cm^{-1} has a shoulder at
431 cm^{-1} which we had not tried to inerpret. We can now
suggest this as the "$\rho_{CF_3}(A'')$" frequency on the basis of
the normal coordinate analysis. The Raman spectra of Smard-
zewski and Fox (5,19) for an Ar matrix shows a single band
at 433 cm^{-1} whose width is comparable to that of other bands
in the Ar matrix. In our opinion their Raman spectra can
neither conform nor deny the possible presence of two
fundamentals separated by a few cm^{-1} here. The liquid Raman
band at 436 cm^{-1} taken to be the counterpart of the bank at

429 cm^{-1} in the IR of the gas is polarized and should be " δ_{COF} ", an A' mode. This 436 cm^{-1} band is slightly asymmetric to low frequencies so a weak depolarized band a few cm^{-1} away from 436 cm^{-1} could possible be present. If one accepts the " τ_{CF_3} ", "$2 \tau_{CF_3}$ ", " $\rho_{CF_3}(A')$ " interpretation of the three bands between 100 and 300 cm^{-1} and the general validity of our force field, then 431 cm^{-1} is the only candidate for the " $\rho_{CF_3}(A'')$ " mode.

For CF_3OCl, there is no evidence of a band at 348 cm^{-1} in either the Raman or IR spectra. The band with a Q branch at 393 cm^{-1} has a small peak at 389 cm^{-1} on its P branch which we assign to ν_4 of the impurity SiF_4 whose presence is confirmed by its ν_3 at 1032 cm^{-1} (39). We don't believe that both 393 and 389 cm^{-1} are two nearly degenerate modes of CF_3OCl as we assigned for 429 and 431 cm^{-1} in CF_3OF. The liquid Raman band at 397 cm^{-1}, taken as the counterpart of the band at 393 cm^{-1} in the IR of the gas, is slightly asymmetric to low frequencies. This could be the natural shape of the band or there could be a small contribution from ν_4 of SiF_4 (a weak Raman band)(39). The shapes of the Raman bands at 436 cm^{-1} in liquid CF_3OF and 397 cm^{-1} in liquid CF_3OCl are sufficiently different that, in our opinion, it is possible that CF_3OF could have 2 bands present and CF_3OCl could have only one band present or one CF_3OCl band and one weak SiF_4 band present. Since the 348 cm^{-1} frequency in our calculation is in the A' block it is most reasonably

associated with the 393 cm^{-1} IR band which must be in the
A' block as it's Raman counterpart at 397 cm^{-1} is polarized.
Then the missing band for " $\rho_{CF_3}(A'')$ " is near 420 cm^{-1} for
our calculation in Table 7 and between 420 and 465 cm^{-1} for
some other calculations we have made. Our Raman data for
CF_3OCl show a very weak band at 430 cm^{-1} in every spectrum
where the sensitivity is set high enough to record the 611
cm^{-1} band, which is the weakest Raman line assigned to a
fundamental " $\delta_{CF_3}(A'')$ ". The baseline in the IR is not flat
in this region due to problems with exact compensation of a
polyethylene band in the gas cell windows with two polyethlene
sheets in the reference beam. It is difficult to be sure
whether there is a very weak band near 430 cm^{-1} in the IR or
not. The fact that the band, if present, is weak compared
to " $\rho_{CF_3}(A')$ " at 233cm^{-1} seems a little surprising for
" $\rho_{CF_3}(A'')$ "; however, it is the only candidate for missing
" $\rho_{CF_3}(A'')$ " mode.

Initially our sample of CF_3Cl contained a large amount
of chlorine and the band in CF_3OCl at 561 cm^{-1} in the Raman
spectrum of the liquid was only visible as a small shoulder
on the intense band due to the chlorine. Purification of the
CF_3OCl sample gave the Raman spectra shown in
Figures 7 and 8. The band at 548 cm^{-1} in Figure 7 and 8
does not appear in the IR spectrum of gaseous CF_3OCl.
Smardzewski and Fox (5,19) observe bands in Raman spectra

of CF_3OCl in an Ar matrix at 547 and 539 cm^{-1} with relative
intensities of 9 and 10, respectively. Our band at 548 cm^{-1}
in the Raman spectrum of liquid CF_3OCl appears to consist of
two overlapping bands of equal intensity at ~551 and ~545 cm^{-1}.
Since all the CF_3OCl fundamentals are reasonably accounted
for, the band(s) at ~548 cm^{-1} must be either a non fundamental
of CF_3OCl or an impurity.

   The assignment of the 548 cm^{-1} band in the liquid Raman
spectrum of CF_3OCl to a difference band is reasonable on a
frequency basis but not on the basis of intensity and
polarization. Using liquid Raman frequencies "$\delta_{CF_3}(A')$" -
"τ_{CF_3}" = 666 - 122 = 544 cm^{-1} in good agreement with 548 cm^{-1}.
However, the transition from (v_{12}=1, all other v_i=0, an A"
state) to(v_5=1, all other v_i=0, an A' state) is a non
totally symmetric transition and should be depolarized. The
548 cm^{-1} band is polarized. The population of (v_{12}=1, all
other v_i=0) is 10-17 % of that of (all v_i=0) for v_{12}=$^{\tau}CF_3$=122
cm^{-1} between 77 and 100°K (estimated range of sample tem-
perature with liquid N_2 in the cold bath of the low temperature
cell). The fact that the 548 cm^{-1} band has 80% of the intensity
of the "$\delta_{CF_3}(A')$" fundamental at 561 cm^{-1} is difficult to
explain for a non fundamental with no apparent Fermi resonance
possibilities and such an unfavorable Boltzmann population
ratio. On both the intensity and polarization basis we feel
that the 548 cm^{-1} band must be due to a species other than

CF_3OCl.

Possible impurities in the ClF used to prepare CF_3OCl by addition to COF_2 are ClF_5 and ClF_3. However, the Raman spectra of liquid ClF_5 (40) and liquid ClF_3 (41) are such that both compounds would be detected by intense bands well separated from any of the CF_3OCl bands in Figures 7 and 8. The source of the 548 cm^{-1} band(s) must be so similar to CF_3OCl that the two cannot be easily separated by physical means. Another possibility is an additional reaction product from the preparation.

For the case of CF_3OF prepared by addition of F_2 to COF_2, CO_2 impurity in the COF_2 leads to the production of some $CF_2(OF)_2$. By anology the addition of ClF to CO_2 might lead to a variety of materials of the general formula $CF_wCl_x(OF)_y(OCl)_z$. Here w, x, y, z may have the values 0, 1, or 2 in various combinations subject to the restrictins that $(w+x) = 2$ and $(y+z) = 2$. For compounds with C-Cl bonds $(x \neq 0)$ and compounds with O-F bonds $(y \neq 0)$, Raman bands should be present that are well separated from any of the CF_3OCl bands in Figures 7 and 8. One that might be less easily detected is $CF_2(OCl)_2$. It is possible to estimate the frequencies for $CF_2(OCl)_2$ from those of CF_3OCl by using differences between CF_3OF and $CF_2(OF)_2$ frequencies. These estimates suggest the $CF_2(OCl)_2$ might have a strong band at 548 cm^{-1} but not no traces of other bands in addition

to those in Figures 7 and 8.

An additional possibility is further reaction of CF_3OCl to form CF_3OClF_2. The CF_3O fragments of both CF_3OCl and CF_3OClF_2 might have indistinguishable spectra and differentiation would depend on vibrations of the ClF_2 fragment. Since ClF_3 has a ClF stretching mode at 529 cm^{-1} (gas phase, with liquid at lower frequency), the ClF_2 fragment of CF_3OClF_2 could be responsible for the 548 cm^{-1} band. However, it is difficult to believe that the remaining modes of the ClF_2 fragment would not produce additional bands in Figures 7 and 8.

Chlorine dissolved in CF_3OCl would be expected to give a band (really three bands for $^{35}Cl_2$, $^{35}Cl^{37}Cl$ and $^{37}Cl_2$) near 545 cm^{-1}. Liquid chlorine in our low temperature cell with liquid nitrogen in the bath gave bands at 547, 540, and 533 cm^{-1} in the intensity ratio 6.5 : 4.5 : 1 (theoretical 9 : 6 : 1). Condensation of chlorine into a CF_3OCl sample of purity similar to Figures 7 and 8 gave bands at 552 and 544 cm^{-1} and a possible shoulder at 537 cm^{-1}. The 548 cm^{-1} band in CF_3OCl cannot be due to chlorine in the same environment as pure liquid chlorine or excess chlorine in CF_3OCl. However, it would be possible for CF_3OCl to form a complex with chlorine of sufficient strength that it si not possible to remove all the chlorine from CF_3OCl. Then the 548 cm^{-1} band could be due to the stretching of the Cl-Cl bond in the

complex.

The observation of this band in the Raman spectra of liquid CF_3OCl near liquid nitrogen temperature and of CF_3OCl in an Ar matrix at $8°K$ but not in the IR spectrum of the gas at room temperature is reasonable. Low temperature favors complex formation and the complex is probably not present in the gas phase at room temperature. Even if the complex were present in the gas it would probably be too weak to cause the IR inactive stretching of gaseous Cl_2 to become observable in the IR spectrum of the gaseous complex.

The proposed complex of chlorine with CF_3OCl might be expected to show isotope splitting in its chlorine stretching mode. Assuming the complexation takes place via the chlorine atom of CF_3OCl (analogous to the X_3^- halide complex ions like I_3^-), eight complexes are possible as follows:

No.	Mass Arrangement $CF_3OCl \ ... \ Cl \ —— \ Cl$			Relative Abundance
1	35	35	35	27
2	35	35	37	9
3	35	37	35	9
4	35	37	37	3
5	37	35	35	9
6	37	35	37	3
7	37	37	35	3
8	37	37	37	1

The effect of the mass of the chlorine atom in CF_3OCl on the frequency for stretching the Cl-Cl bond from Cl_2 in the complex depends on the strength of the complex. The limit for a weak complex could be three bands due to three degenerate sets as follows: 1 and 5 of relative intensity 36; 2, 3, 6, and 7 of relative intensity 24; and 4 and 8 of relative intensity 4. As complex strength increases these degeneracies would be broken as the mass of the chlorine atom in CF_3OCl begins to influence the frequency. A reasonable extreme would be where the vibration is still best treated as a perturbed diatomic molecule stretching rather than a three body problem with antisymmetric and symmetric skeletal stretching and skeletal bending. However, the degeneracies are broken and the eight frequencies might tend to group into the following four bands: 1 of relative intensity 27; 2, 3, and 5 of relative intensity 27; 4, 6, and 7 of relative intensity 9; and 8 of relative intensity 1.

For the weak extreme, the third band probably would not be observed as it is too weak so a higher frequency band 1.5 times as intense as a lower frequency band is to be expected. For the strong extreme the fourth band would definitely be too weak to observe and the extent of overlap of the other three bands is uncertain. A likely result would be that the third band of intensity 9 would overlap the second band of intensity 27 to give a single asymmetric band or a

band with a low frequency shoulder. This superposition
would result in a lower frequency band with relative intensity
27 (or more from overlap of the third band) and a higher
frequency band of relative intensity 27 (from complex 1).
Thus, two resolvable bands seem reasonable for the range
of complex strengths suggested. The higher frequency band
would be expected to be from 1.5 times as intense to slightly
less intense than the lower frequency band depending on the
strength of the complex.

The formation of a $CF_3OCl \ldots Cl$—Cl complex will then
account for a band at 548 cm^{-1} in the Raman spectrum of liquid
CF_3OCl appearing to consist of two overlapping bands of equal
intensity at 551 and 545 cm^{-1}. The observation by Smardzewski
and Fox (5,19) of bands at 547 and 539 cm^{-1} with relative
intensities of 9 and 10, respectively, in the Raman spectrum
of CF_3OCl in an Ar matrix is also consistent. The conditions
of a liquid near 77°K and an Ar matrix at 8°K are conditions
that should favor complex formation. The improved resolution
in the Ar matrix is also reasonable.

This discussion is, of course, speculative and does not
prove anything. However, this explanation does account for
the fact that no additional unexplained bands are found. We
believe it is unreasonable to associate the 548 cm^{-1} band
with pure CF_3OCl. Thus some other species must be responsible.
At present, the $CF_3OCl \ldots Cl$—Cl complex provides the

simplest explanation and we consider it the most likely
cause of the ~548 cm^{-1} band.

      C.   Comments on the L^{-1} Matrices and the Normal
             Coordinates

     The matrix L^{-1} (eigenvector inverse matrix) gives the
transformation between symmetry and normal coordinates:
$Q = L^{-1}S$. These transformation matrices for both the A' and
A" symmetry species of CF_3OF and CF_3OCl are shown in Tables
10 and 11, respectively, for the calculation with $(1/\lambda_i^2)$
weighting. Thus, Q_1 essentially equals approximately $2\ S_1$
and Q_9 approximately $2\ S_{10}$ for both molecules. Thus they are
described as the antisymmetric stretches of the CF_3 group
for the A' and A" symmetry species, respectively. In gen-
eral the L^{-1} matrices in Tables 10 and 11 show a large amount
of mixing of symmetry coordinates to be present in the normal
coordinates. For example in CF_3OF we have Q_3(947 cm^{-1}) $\cong$
3.39 S_2 + 1.63 S_7 and in CF_3OCl Q_3(919 cm^{-1}) $\cong$ 3.73 S_2 +
1.82 S_7. Thus, the normal coordinate Q_3, assigned as the CO
stretching mode, has important contributions from both
symmetrical CF_3 stretching and the CO stretching motions.
This situation is not unreasonable when one considers the
relative masses of the carbon and three fluorine atoms of
the CF_3 group. A stretching of the C-O bond would tend to
shorten the C-F bonds in a symmetrical manner. The resemblance
of the form of normal coordinates called CO stretching mode

Table 10. Symmetrized L^{-1} Matrix for CF_3OF[a]

	S_1	S_2	S_3	S_4	S_5	S_6	S_7	S_8	S_9	S_{10}	S_{11}	S_{12}	S_{13}
Q_1	1.69	-0.18	0.26	0.28	0.16	-0.44	0.66	-0.14					
Q_2	0.90	1.07	-0.51	0.12	-0.55	-0.02	-1.26	-0.03					
Q_3	-0.80	3.39	0.84	0.00	0.08	-0.47	1.63	-0.18					
Q_4	-0.71	-1.44	2.18	0.15	-0.36	-0.30	-0.81	-0.46					
Q_5	-1.43	-1.67	-1.77	0.57	-1.77	-1.15	1.30	-0.32					
Q_6	-2.45	0.45	-0.76	2.45	1.09	-0.06	-1.29	-0.62					
Q_7	0.74	0.09	2.25	1.67	-1.45	2.04	2.44	1.63					
Q_8	0.84	-0.29	-0.07	0.01	1.18	-3.97	-2.85	3.73					
Q_9										2.11	0.32	-0.15	0.00
Q_{10}										-2.91	2.35	-1.19	0.02
Q_{11}										0.55	1.84	2.58	-0.07
Q_{12}										0.87	0.27	2.13	1.29

a. See footnote a in Table 6 for numbering system for S_i and Q_i.

Table 11. Symmetrized L^{-1} Matrix for CF_3OCl[a]

	S_1	S_2	S_3	S_4	S_5	S_6	S_7	S_8	S_9	S_{10}	S_{11}	S_{12}	S_{13}
Q_1	1.87	-0.06	0.06	0.29	0.10	-0.38	0.40	-0.14					
Q_2	0.46	1.01	0.01	0.07	-0.61	-0.05	-1.37	-0.05					
Q_3	-0.27	3.73	-0.29	-0.05	0.21	-0.17	1.82	0.03					
Q_4	-1.68	0.20	1.94	0.43	0.09	-0.96	0.09	-0.77					
Q_5	-1.00	-1.63	-0.93	0.45	-2.10	-0.74	1.83	-0.21					
Q_6	-2.19	0.23	-1.09	2.67	0.70	0.26	-0.96	-0.26					
Q_7	-1.26	0.23	3.59	1.30	-1.29	1.63	2.39	2.29					
Q_8	0.55	-0.43	-1.37	-0.38	1.42	-5.61	-3.14	3.88					
Q_9										2.10	0.32	-0.15	0.00
Q_{10}										-2.90	2.40	-1.12	0.02
Q_{11}										0.63	1.79	2.59	-0.08
Q_{12}										0.88	0.18	2.58	1.50

a. See footnote a in Table 6 for numbering system for S_i and Q_i.

in both CF_3OX molecules tends to support the correctness
of the new assignment of this mode. It can been seen that
the chief contribution to the normal coordinates came from
the related symmetry coordinates in some cases. Then the
word description of the mode such as 'antisymmetric CF_3
stretching' is still qualitatively correct. However some
modes involve extensive mixing of the symmetry coordinates
and the word descriptions do not have even qualitative
significance.

D. Comments on the Potential Energy Distribution

Another method of describing molecular vibrations is
through the potential energy destribution (PED) which is
obtained from the L matrix (eigenvector matrix). The PED
provides a convenient means for representing the contributions
to the potential energy of the system from the symmetry or
internal coordinate.

Tables 12 and 13 show the degree of localization of a
particular normal mode coordinate among the various symmetry
force constants. In general, the results parallel those of
the L^{-1} matrices in the behavior of mixing, but the distri-
butions show much greater localization than do the L^{-1}
matrices. The most conspicuous examples are from the torsional
modes of both molecules. In this case about 95% of the
contribution is from the torsional force constant.

Table 12. Potential Energy Distribution[a] for CF_3OF

ν_i	F_1	F_2	F_3	F_4	F_5	F_6	F_7	F_8	F_{10}	F_{11}	F_{12}	F_{13}
1	1321	<u>76</u>			16	5	11	12	10				
2	1214	17	38			38		<u>54</u>					
3	941	5	<u>60</u>	7			8	8					
4	883	6		<u>76</u>		5	5	18	7				
5	674	6	6	12		<u>36</u>	17	11					
6	589	5			<u>61</u>	12							
7	420			8	24	10	21	5	<u>29</u>				
8	267						38	6	<u>58</u>				
9	1256									<u>105</u>	20	12	
10	616									8	<u>55</u>	15	
11	429										31	<u>76</u>	
12	128												<u>96</u>

a. Contributions of less than 5% are not included in this table. Numbering of symmetrized force constants F_i follows the numbering of symmetry coordinates in Table 4. No F_9 appears because S_9 is the redundant symmetry coordinate in the A' symmetry block. The numbering of frequencies is from Table 6. See footnote a in Table 6 for the numbering system for ν_i and S_i.

Table 13. Potential Energy Distribution^a for CF$_3$OCl

ν_i		F_1	F_2	F_3	F_4	F_5	F_6	F_7	F_8	F_{10}	F_{11}	F_{12}	F_{13}
1	1309	89			18		9	5	10				
2	1208	5	41			46		67					
3	935		65					16					
4	774	9		51			22		14				
5	658		5	9		48	8	15					
6	571			8	73	5	9						
7	348			30	12	6	50		38				
8	217								44				
9	1262									104	20	11	
10	613									8	51	13	
11	422										30	77	
12	108											5	96

a. Contribution of less than 5% are not included in this table. Numbering of
symmetrized force constants F_i follows the numbering of symmetry coordinates
in Table 4. No F_9 appears because S_9 is the redundant symmetry coordinate
in the A' symmetry block. The numbering of frequencies is from Table 7. See
footnote a in Table 6 for the numbering system for ν_i and S_i.

E.   Comments on the Barrier to Internal Rotation

It is possible to calculate the height of the threefold barrier hindering internal rotation in CF_3OX molecules from the proposed geometry listed in Table 3 and from the observed torsional frequencies. Since the torsional frequencies were below the low frequency limit of the Perkin-Elmer Model 180 infrared spectrophotometer in our laboratory, their values were obtained from the gas phase and liquid Raman data which are discussed in Table 9.

The frequencies 144 cm^{-1}, 122 cm^{-1}, 127 cm^{-1}, and 108 cm^{-1} seem unexpectedly low for rocking vibrations and unexpectedly high for torsions. Eleven of the twelve fundamentals for a CF_3OX structure are reasonably assigned to Raman bands at frequency shifts greater than 200 cm^{-1} for both CF_3OF and CF_3OCl. These four frequencies must then be assigned to the CF_3 torsion mode, but the question is open as to whether the transitions responsible for the bands have $\Delta v = 1$ or $\Delta v = 2$. For a CF_3OX structure of C_s symmetry, as deduced from electron diffraction for CF_3OF (13), $\Delta v = 2$ transitions are totally symmetric while $\Delta v = 1$ transitions are non-totally symmetric for a non-totally symmetric mode such as the CF_3 torsion. Observation of a small depolarization ratio would eliminate a $\Delta v = 1$ transition while a band which is too weakly polarized to be distinguished from being depolarized could be either a $\Delta v = 1$ or $\Delta v = 2$ transition.

For liquid CF_3OF and CF_3OCl where depolarization ratios were measured for the 144 cm^{-1} and 122 cm^{-1} bands, a definite distinction between the bands being weakly polarized and depolarized could not be made.

The microwave spectrum of CF_3OF has been analyzed by Buckley and Weber (6). Vibrational satellites were observed at 194°K and the intensity ratio of the satellite line to the ground state line was about 0.4. This ratio leads to a torsional barrier of 3.9 kcal/mole in reasonable agreement with 4.4 kcal/mole using the 0 –> 1 assignment for the 127 cm^{-1} band in gaseous CF_3OF. Working in the opposite direction, the gaseous frequency of 127 cm^{-1} for CF_3OF at 194°K gives a vibrational state population ratio of 0.39 in excellent agreement with the observed ratio of 0.4. If the 127 cm^{-1} band were 0 –> 2 in the CF_3 torsion then 0 –> 1 would be at 65 cm^{-1} giving a vibrational state population ratio of 0.62 at 194°K. The difference in the ratios of 1.6 (i.e., 0.62/0.39) seems to exceed any possible experimental error in measuring the intensity ratio. Once the decision is made that the observed Raman band is the 0 –> 1 transition, then this frequency is a more reliable source of the barrier height on the grounds that a frequency should be more accurately known than an intensity ratio. Thus we would propose the best value of the barrier for the CF_3 torsion in CF_3OF as 4.4 kcal/mole. For CF_3OCl assuming the same

percentage frequency shift on phase change as CF_3OF, the liquid Raman frequency of 122 cm^{-1} becomes 108 cm^{-1} for the vapor and the barrier for CF_3 torsion is 4.2 kcal/mole.

The barrier heights, V_3, of the CF_3 rotor were calculated following the procedures developed by Fateley and Miller (42-44). The parameters used for this calculation are listed in Table 14. Agreement between the two values of the barrier height in the two molecules in the same phase is good. These values are slightly higher than the microwave result of 3.9 kcal/mole (13). A band at 56 cm^{-1} was assigned as the 0 -> 1 transition of the CF_3 torsion and a potential barrier of 395 cm^{-1} (1.13 kcal/mole) was determined with an assumed geometry by Wilt and Jones (4). The existence of this band is questionable based on our IR and Raman data and the Raman data of Smardzewski and Fox (5). This strikingly low value for the barrier height is also inconsistent with the microwave and electron diffraction results.

Table 14. Summary of Parameters in Barrier Height
Calculation

Parameter	CF$_3$OF		CF$_3$OCl	
	Raman gas	Raman liquid	Raman gas	Raman liquid
τ_{CF_3} (cm^{-1})	127	144	108[a]	122
$I\alpha$ (amu-Å^2)[b]	88.06	88.06	88.06	88.06
rI_α (amu-Å^2)[b]	13.85	13.85	18.40	18.40
$\Delta b_{v\sigma}$ [c]	46.37	52.58	52.40	59.19
S [c]	560.8	718.3	713.4	906.3
F(amu-Å^2)	1.217	1.217	0.916	0.916
V_3(kcal/mole)[c]	4.4	5.6	4.2	5.3

a. Calculated assuming the same percentage frequency shift
    on phase change as CF$_3$OF.

b. The quantity rI_α , the reduced moment for internal rotation,
    is given by

$$rI_\alpha = (1 - I_\alpha \sum_{i=1}^{3} \lambda_i / I_i) I_\alpha$$

    here I is the moment of interia of the CF$_3$ group about
    its symmetry axis, I_i and λ_i are the principal moments
    of inertia of the entire molecule and direction cosines
    of the CF$_3$ symmetry axis with respect to the principal
    axes, respectively.

c. The equations used to calculate V_3(cm^{-1}) are as follows:

$$\tau_{CF_3} = \Delta E_{v\sigma} = (2.25) F \Delta b_{v\sigma}$$

$$F = 16.8576/ rI_\alpha \text{ (amu-Å}^2)$$

$$V_3 = 2.25 \text{ FS (cm}^{-1})$$

    The Mathieu function table of $b_{v\sigma}$ (the eigenvalue of the
    Mathieu equation) VS. S (the dimensionless parameter) used
    is from reference (44).

II. RAMAN SPECTRA OF $CF_2(OF)_2$ AS A FUNCTION OF TEMPERATURE

CHAPTER I
INTRODUCTION

Cady and co-workers were the first to report the
preparation of a carbon-containing hypofluorite, CF_3OF (11).
Since then a number of new carbon containing -OF compounds
have been reported (45). Bis(fluoroxy)perfluoroalkanes
are a new class of compounds coming from this development.
Bis(fluoroxy)difluoromethane, $CF_2(OF)_2$, is the parent member
of this class (46). It is conveniently prepared in high yield
by static, cesium fluoride catalyzed fluorination of carbon
dioxide (47).

The longer known hypofluorite, CF_3OF, undergoes a
variety of interesting reactions with both inorganic and
organic reagents. The spectroscopic investigations and
intramolecular force field calculation of this compound are
reported in Part I of this study.

Because of the apparent similarity of $CF_2(OF)_2$ and
CF_3OF, it was of interest to study the physical properties
of this compound by using vibrational spectroscopy.

Structural investigation of $CF_2(OF)_2$ by the analysis
of its fluorine nuclear magnetic resonance spectrum suggested
that the two triplets (1:2:1) of equal area at -155.7 and
+81.7 ppm (trichlorofluoromethane was the internal reference)
be assigned to the two equivalent OF and CF fluorines, res-

pectively (46,47). A somewhat detailed infrared spectrum of $CF_2(OF)_2$ was reported by Mitchell and Merrit (48). Measured frequencies of the observed infrared bands (in cm^{-1}) of this compound were presented. A possible C_{2v} symmetry with 15 fundamental vibrations was suggested.

During the course of this study, the concept of rotational isomerism was proposed to explain the observation of more bands in the low temperature liquid Raman spectrum of this molecule than what would be allowed by the selection rules for a single spatial structure. The additional bands could not assigned to overtone or combination modes and could only be satisfactorily explained on the basis of this compound possessing more than one geometric structure.

A subsequent study of the temperature effect on Raman spectra confirmed this proposition, as the spectra of this molecule were temperature sensitive. Certain bands became decidedly weaker and some became much stronger when the temperature of this sample was increased from near liquid nitrogen temperature ($-196^{o}C$) up to above its boiling point ($-40^{o}C$).

This observation may be rationalized in terms of a depopulation of a thermodynamically less stable isomeric structure with decreasing temperature. The molecules may exist as an equilibruim mixture of two or more rotational isomers or conformers over a temperature range. In the present

study we have assumed a two isomer mixture although the possibility of more than two isomers being present cannot be rigorously excluded.

The experimental determination of absolute Raman intensity was known to be very difficult. Consequently a relative intensity comparision was used to observe the population change.

The present report concerns preliminary work on this subject. The vibrational spectra of this compound were recorded and tentative interpretation is presented. More experimental data are needed to fully explore the dynamic nature of this conformational system. To this end some suggestions for further study involving other spectroscopic techniques are presented.

CHAPTER II
EXPERIMENTAL

The samples of bis(fluoroxy)perfluoromethane, $CF_2(OF)_2$, used in this atudy were prepared by Dr. D. D. DesMarteau at Kansas State University. The preparation was that of Hohorst and Shreeve (47), and involved the static fluorination of carbon dioxide with excess fluorine in the presence of cesium floride. The crude sample was trapped at liquid nitrogen temperature and then purified by gas chromatography. The purity of this sample was monitored by recording its infrared spectrum. The infrared spectrum of this sample shown in Figure 13 is similar to that reported by Thompson (46) and Mitchell and Merrit (48). The spectrum shown in Figure 14 does not appear to agree as well with that of Thompson (46) but is qualitatively similar to that of Mitchell and Merrit (48).

The infrared spectra were recorded using procedures described in the experimental section in Chapter II, Part I of this thesis. Liquid Raman spectra were recorded in a low temperature cell similar in design to that of Brown et.al.(18) on a system for Laser Raman spectroscopy consisting of a Spex Model 14018 Double Monochromator with a RCA C31034 photomultipler tube and Princeton Applied Research Model 1140AC Quantum Photometer. Excitation was with the 5145 Å line of a Spectra-Physic Model 164-03 argon ion laser. A complete description of the system for Laser Raman spectroscopy appears elsewhere (8).

EXPLANATION OF FIGURE 13

Gas-phase Infrared Spectrum of $CF_2(OF)_2$
in the Region 3000-300 cm^{-1}.

Spectrometer: Perkin-Elmer Model 180

Sampling Method: 5 cm Path Length Cell

with AgCl Windows

Pressure: 240 mm Hg

Energy Mode: Constant I_o

Resolution: 2.0 cm^{-1} at 4000 cm^{-1}

Gain: 6

Slit Program: 5

Time Constant: 1

Scan Time: Fine 5, Coarse 10

Suppression: 5

Temperature: $25^o C$

By means of appropriate coolants, the low temperature
cell was used to record the liquid Raman spectrum with the
cell bath at four different temperatures of $-40^{\circ}C$, $-78^{\circ}C$,
$-135^{\circ}C$, and $-196^{\circ}C$. Liquid nitrogen was used as coolant to
get the bath temperature down to $-196^{\circ}C$. The $-135^{\circ}C$ temperature
was obtained by using a dry ice-freon 12-liquid nitrogen bath.
Constant liquid nitrogen addition followed by vigorous stirring
(to break the ice layer) was required to keep temperature
within $135 \pm 2^{\circ}C$. A dry ice-freon 12 mixture was used to get
the bath temperature within $1^{\circ}C$ of $-78^{\circ}C$. A freon 12-liquid
nitrogen bath was used for the temperature of $-40\pm1^{\circ}C$. The
normal boiling point of $CF_2(OF)_2$ is $-64^{\circ}C$ which is below the
experimental bath temperature of $-40^{\circ}C$. After long irradiation
with the incident laser beam, bubbles, which were probably
caused by local heating with subsequent vigorous vaporization,
come up during the recording. These bubbles may have produced
some fluctuation in the scattered light. With the loss of
sample through constant vaporization, the effect on signal
intensities and depolarization ratios is hard to estimate.

The spectrum of the gas was obtained with the sample
contained in a cell similar in design to the standard Spex
multipass gas cell. High laser power and high gain were re-
quired for recording the gas phase Raman spectra. Due to this
experimental difficulty, the gas phase Raman spectrum (Figure
15) was not as good in quality as the liquid Raman spectrum.
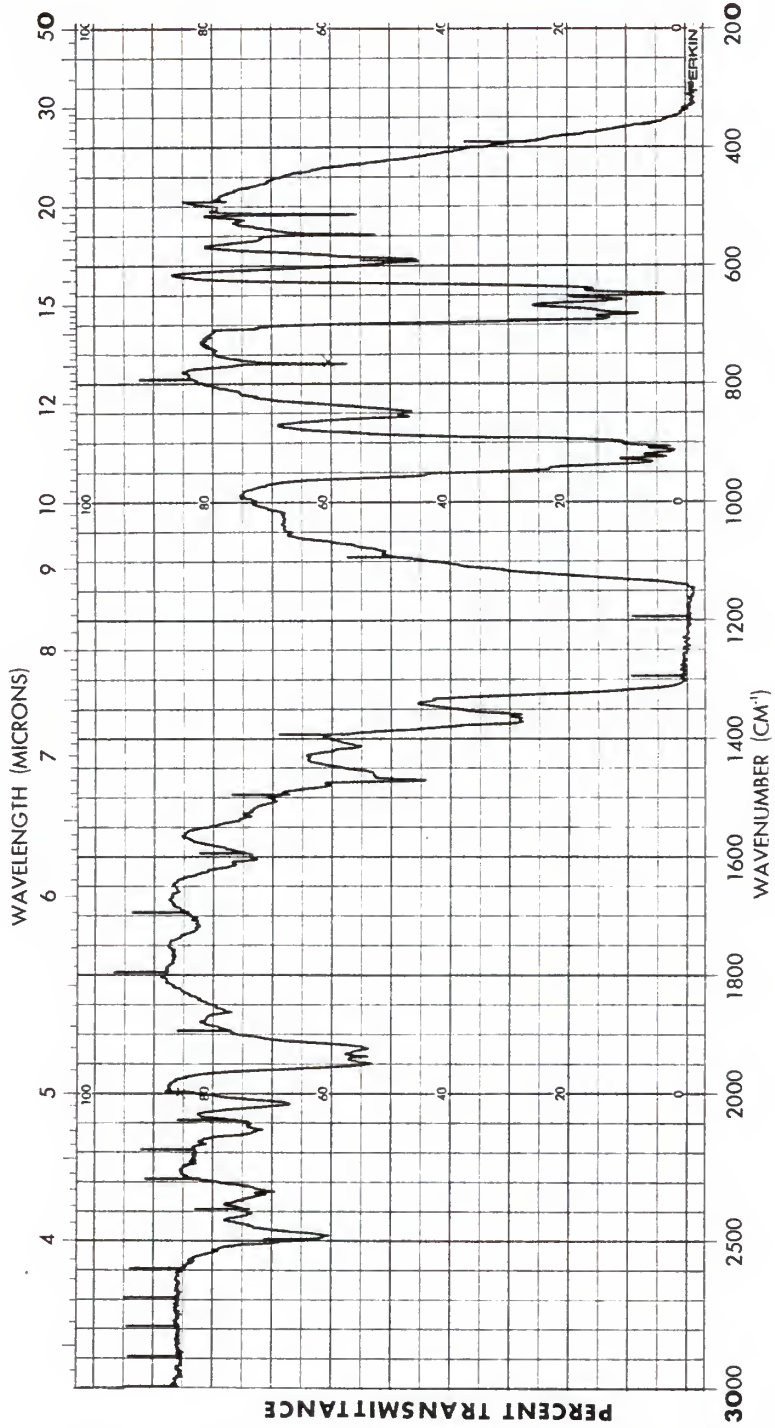
EXPLANATION OF FIGURE 15

Raman Spectrum of Gas-phase $CF_2(OF)_2$

in the Region 1000-800 cm^{-1}

Spectrometer: Spex Model 14018

Slit Setting: 200 mμ
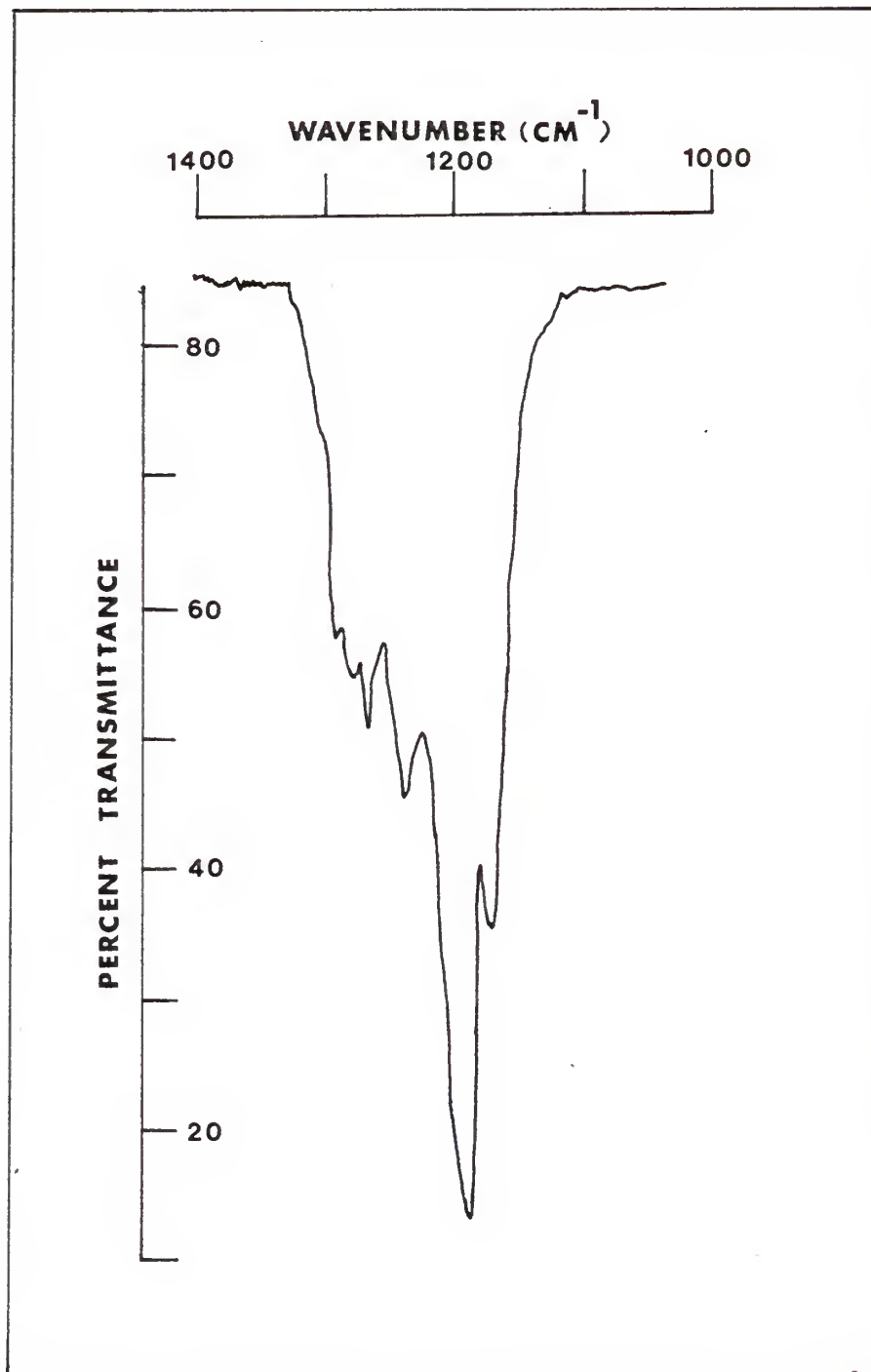
Gain: 300

Filter: 2.2%

Scan Speed: 0.5 cm^{-1}/sec

Chart Speed: 3 cm/min

Source: Ar^+ Laser at 5145 Å

Power: 1.4 W

Temperature: 25°C

Pressure:~ 600 mm Hg
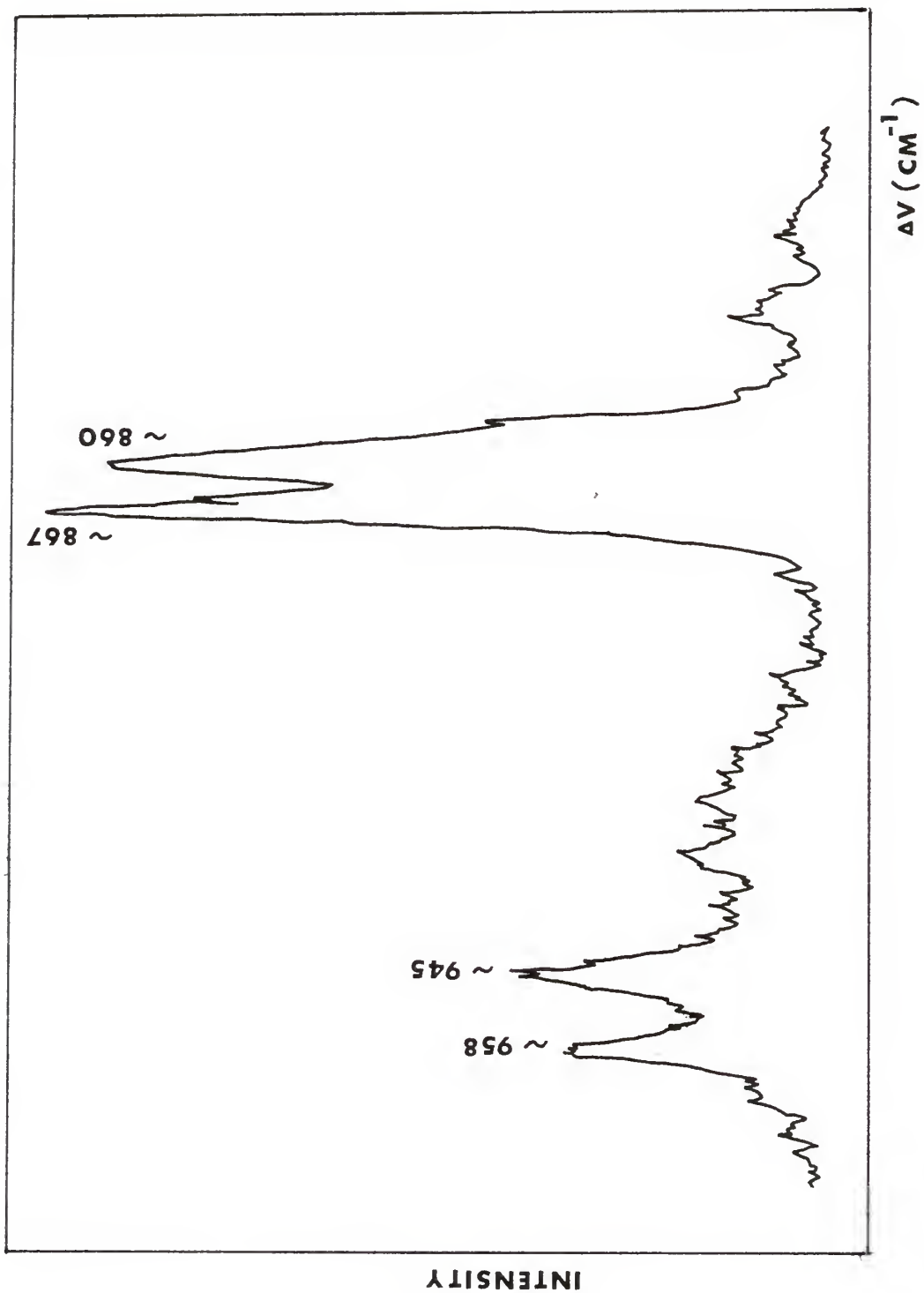
CHAPTER III
RESULTS AND DISCUSSION

A. General

No detailed structural studies like electron diffraction
or microwave spectroscopy have been published for the molecule
$CF_2(OF)_2$. A F-19 nuclear magnetic resonance study has in-
dicated that this molecule has two equivalent -OF groups
and that the two fluorine atoms of the $-CF_2-$ group are
equivalent as well (46,47). This NMR study was performed
at ambient temperature using a 10% solution of this compound
in trichlorofluoromethane, which also served as the internal
reference. It is not clear what the influence of the solvent
on the conformer equilibrium might be.

An inspection of the Raman spectrum of liquid $CF_2(OF)_2$
in Figure 16 shows at least 22 well-defined Raman bands with
some additional shoulders. If one assumes only one molecular
configuration, either with C_{2v} symmetry as indicated by the
NMR study or C_s symmetry as compared with CF_3OF, then the
maximum number of bands that should be observed is 15, which
is the total number of normal vibrations for the $CF_2(OF)_2$
molecule. Difference bands can be ruled out because of the low
bath temperature used to record the Raman data. One is then
forced to look for combination or overtone bands to explain the
"extra" Raman bands.

For example the 524 cm^{-1} band could be explained as
arising from the combination, $243 + 280 = 523$ cm^{-1}, but the
524 cm^{-1} Raman band is as intense as the 280 cm^{-1} band.

EXPLANATION OF FIGURE 16

Raman Spectrum of Liquid $CF_2(OF)_2$

Spectrometer: Spex Model 14018

Slit Setting: 200 μm

Gain: 3 K

Filter: 1.3%

Scan Speed: 1 cm^{-1}/sec

Chart Speed: 3 cm/min

Source: Ar^+ Laser at 5145 Å

Power: 300 mW

Temperature: $-196^{\circ}C$

Therefore, it is unlikely to be a combination band on the
basis of its intensity relative to the fundamentals from
which it would have to arise. One is then forced on the basis
of the Raman spectrum alone to consider a second rotational
isomer or conformer as being present at -196°C. Then, the
additional Raman bands could arise from this second species.
The effects of temperature on the Raman spectrum of $CF_2(OF)_2$
in the liquid state were observed at four different bath
temperatures: -40°C, -78°C, -135°C and -196°C. In the present
study, the intensities of the Raman bands at 944 and 867 cm^{-1}
have been found to increase, as temperature is raised, re-
lative to intensities of other bands. Also a decrease in
intensity of the band at 933 cm^{-1} is observed. Since so many
bands vary in intensity with temperature, a second conformer
is a logical choice for the interpretation of this spectroscopic
results. The less stable conformer favored at high temperatures
is designated as the high energy conformer; the more stable
one favored at low temperatures will be called the low energy
conformer.

B. Intensity Considerations

The intensity of Raman bands is dependent on many factors
and may be influenced by sampling methods as well as instrumental
and molecular effects. New coolant and fresh sample are needed
for each different temperature. Also the positions of the low

EXPLANATION OF FIGURE 17

Raman Spectrum of Liquid $CF_2(OF)_2$

Spectrometer: Spex Model 14018

Slit Setting: 150 μm

Gain: 3 K

Filter: 1.3%

Scan Speed: 1 cm^{-1}/sec

Chart Speed: 3 cm/min

Source: Ar^+ Laser at 5145 $\overset{o}{A}$

Power: 300 mW

Temperature: $-135^{\circ}C$

EXPLANATION OF FIGURE 18

Raman Spectrum of Liquid $CF_2(OF)_2$

Spectrometer: Spex Model 14018

Slit Setting: 200 μm

Gain: 3 K

Filter: 1.3%

Scan Speed: 1 cm^{-1}/sec

Chart Speed: 3 cm/min

Source: Ar^+ Laser at 5145 $\overset{o}{A}$

Power: 300 mW

Temperature: $-78^{o}C$

EXPLANATION OF FIGURE 19

Raman Spectrum of Liquid $CF_2(OF)_2$

Spectrometer: Spex Model 14018

Slit Setting: 150 μm

Gain: 3 K

Filter: 1.3%

Scan Speed: 3 cm^{-1}/sec
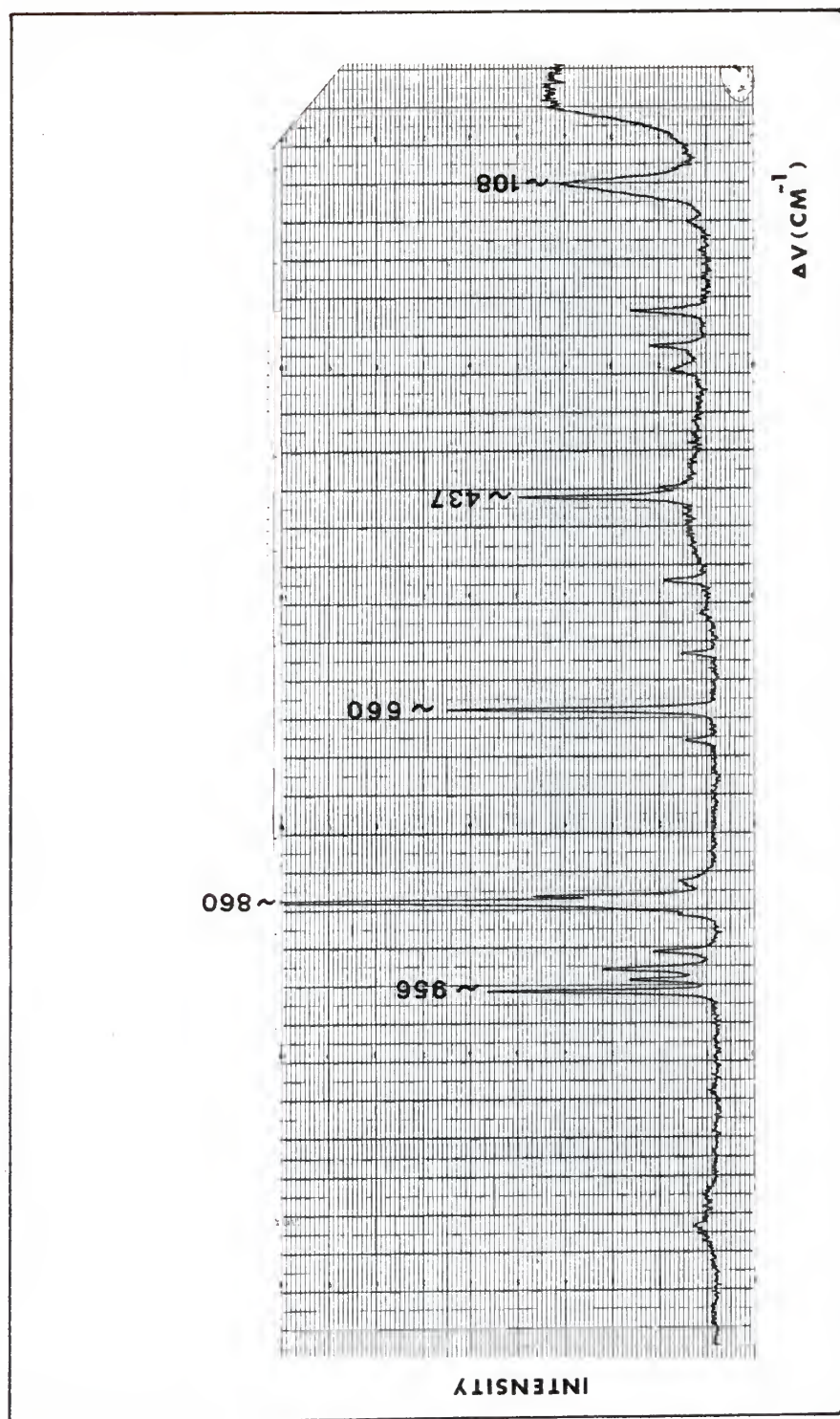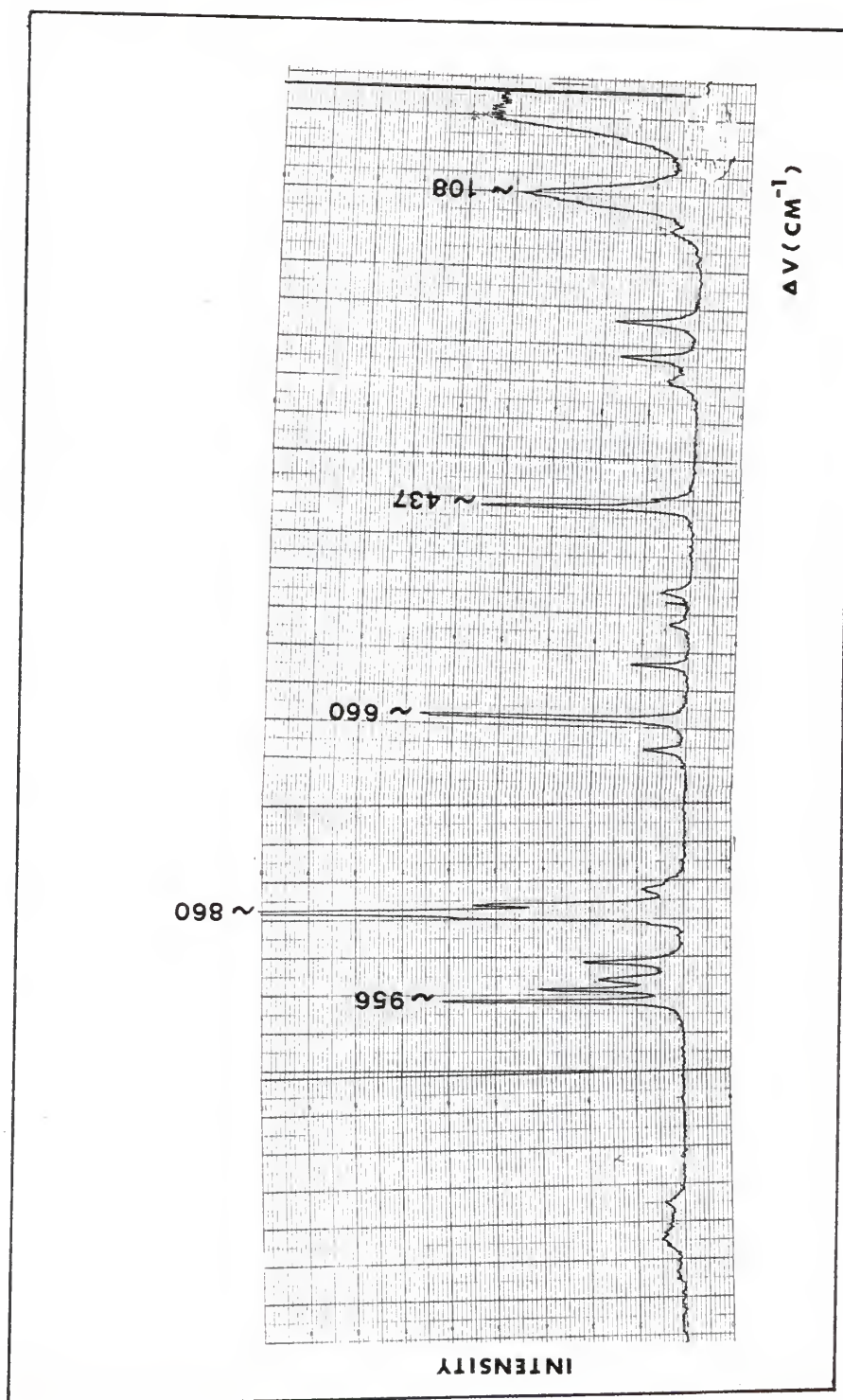
Chart Speed: 3 cm/min

Source: Ar^+ Laser at 5145 $\overset{o}{A}$

Power: 300 mW

Temperature: $-40^{\circ}C$
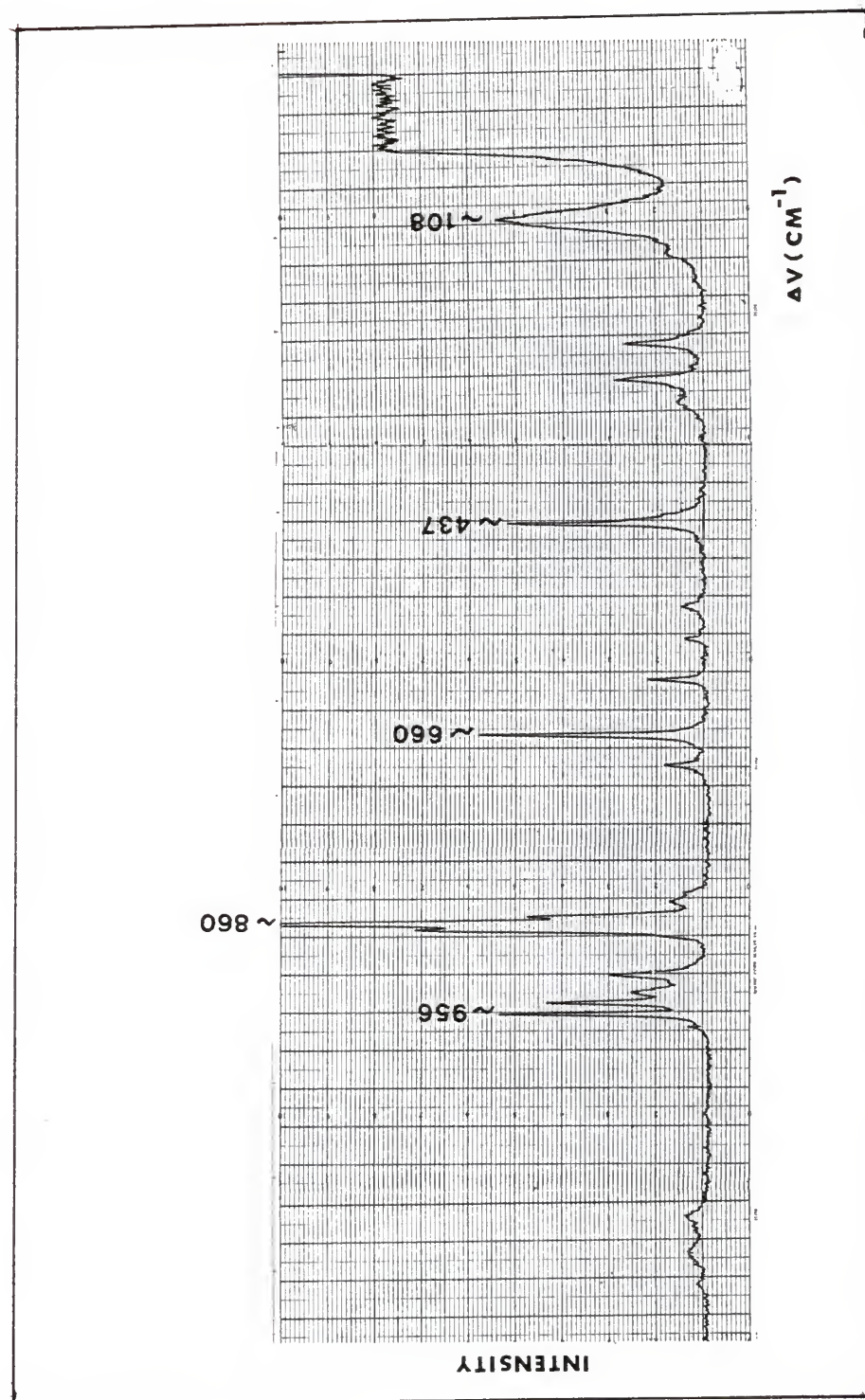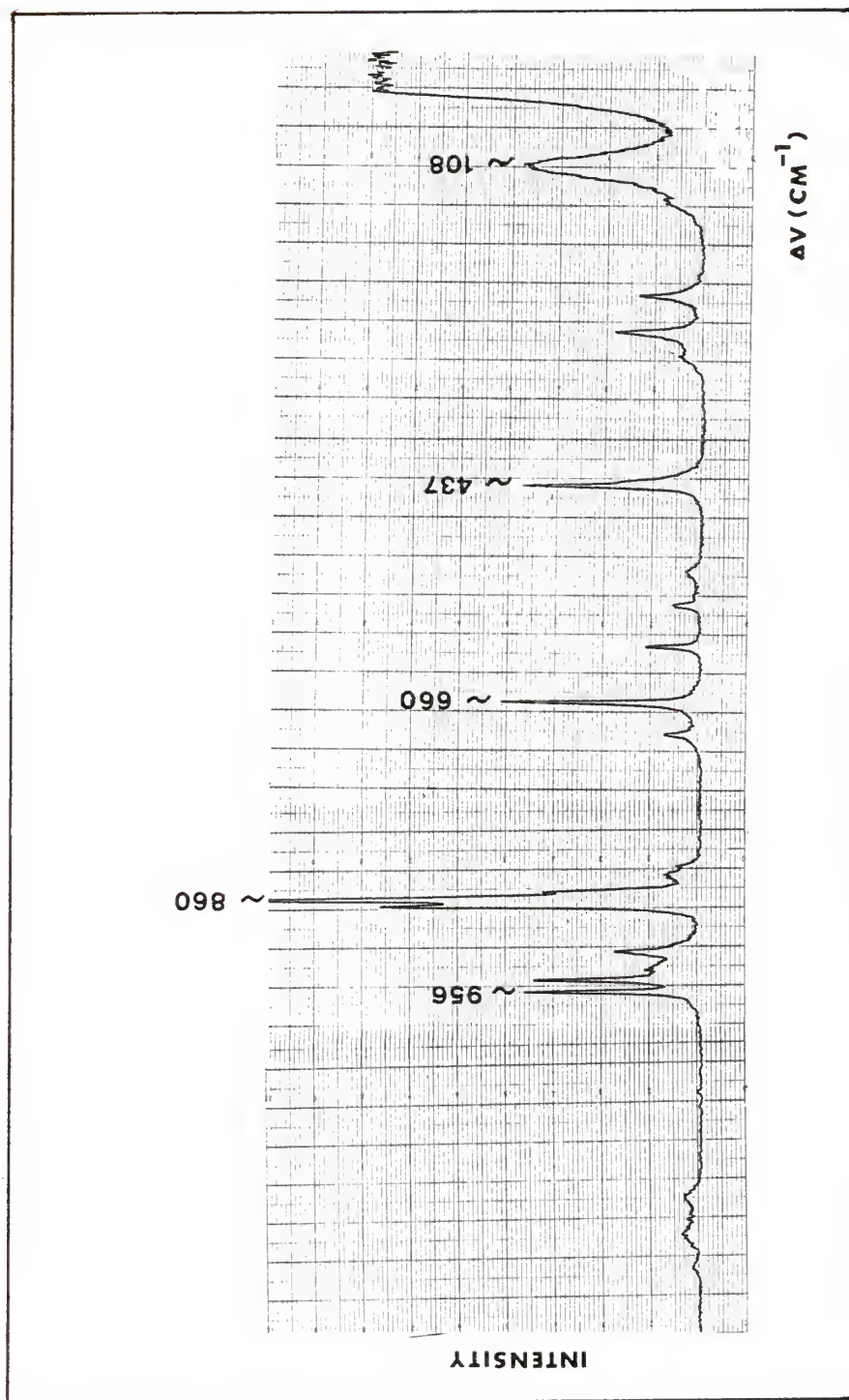
Table 15. Relative Intensities[a] of the Bands from
Liquid Raman Spectra $CF_2(OF)_2$

Freq.[b] (cm^{-1})	Temperature (^{o}C)			
	-40	-78	-135	-196
108	34.8	36.8	28.0	29.5
147	4.4	6.7	4.9	6.4
243	13.2	14.1	13.0	18.0
280	16.8	16.1	12.1	14.2
304	4.0	5.0	4.9	9.2
428	6.8	8.0	6.4	12.5
434	15.2	15.4	11.3	15.3
437	37.6	36.1	32.7	41.0
524	2.8	4.0	4.6	10.9
559	6.0	5.0	3.2	4.4
602	12.4	11.4	9.0	6.8
660	42.8	44.5	41.3	49.5
692	7.6	8.0	6.6	5.8
827	4.8	4.0	2.9	2.7
837	6.4	6.7	6.4	6.8
854	33.2	33.4	32.4	32.9
860	100.0	100.0	100.0	100.0
867	64.8	50.8	35.8	20.0
874	6.8	7.7	5.8	6.4
914	17.6	17.7	15.6	12.9
933	10.4	13.0	13.3	20.0
944	34.8	30.8	22.5	16.9
956	38.8	39.1	37.3	42.7
1060	1.2	1.3	0.6	2.0
1170	3.4	3.7	3.2	3.4
1192	2.2	2.7	3.5	3.0
1207	3.2	3.0	3.8	4.1
1240	1.8	1.7	1.5	1.7

a. The peak height of the Raman band at 860 cm^{-1} was taken
to be 100 for each temperature.

b. The frequencies listed are the average values of the
frequencies measured at the four temperature.

temperature cell as well as the spectrophotometer tuning may not be the same for each experiment. This means the experimental determination of absolute Raman intensities is difficult. Many corrections and calibrations are necessary before intensity values are obtained that can be used to derive molecular properties.

An approximate correction for these errors can be made by using an internal or external standard. However, with an external standard it is difficult to obtain geometrical accuracy even when using the same cell and with internal standards, the intensity of the standard may vary with environmental changes. Relative intensities can, of course, be measured (49).

We measured Raman liquid spectra at bath temperatures of -196, -135, -78, and -40°C shown in Figures 16, 17, 18 and 19, respectively. Peak heights of the bands were used as a measure of the intensity of the Raman bands. Every height was normalized to a height of 100 for the most intense band which is near 860 cm^{-1} at each temperature. Table 15 contains the relative intensity data measured from a 10X abscissa expansion spectrum. Thus, the relative intensities of the bans were used as a measure of the relative concentration of the indicated conformer. Figures 20 and 21 show the effect of temperature on the relative intensities in the CO and OF stretching regions.

EXPLANATION OF FIGURE 20

Effect of Temperature on the Raman Spectrum
of Liquid $CF_2(OF)_2$ in the Range 1000-900 cm^{-1}

Spectrometer: Spex Model 14018

Slit Settings: 200 μm at -196 and -78°C

                150 μm at -135 and -40°C

Gain: 3 K

Filter: 0.71%

Scan Speed: 0.2 cm^{-1}/sec

Chart Speed: 3 cm/min

Source: Ar^+ Laser at 5145 Å

Power: 300 mW

Temperature: -196, -135, -78 and -40°C
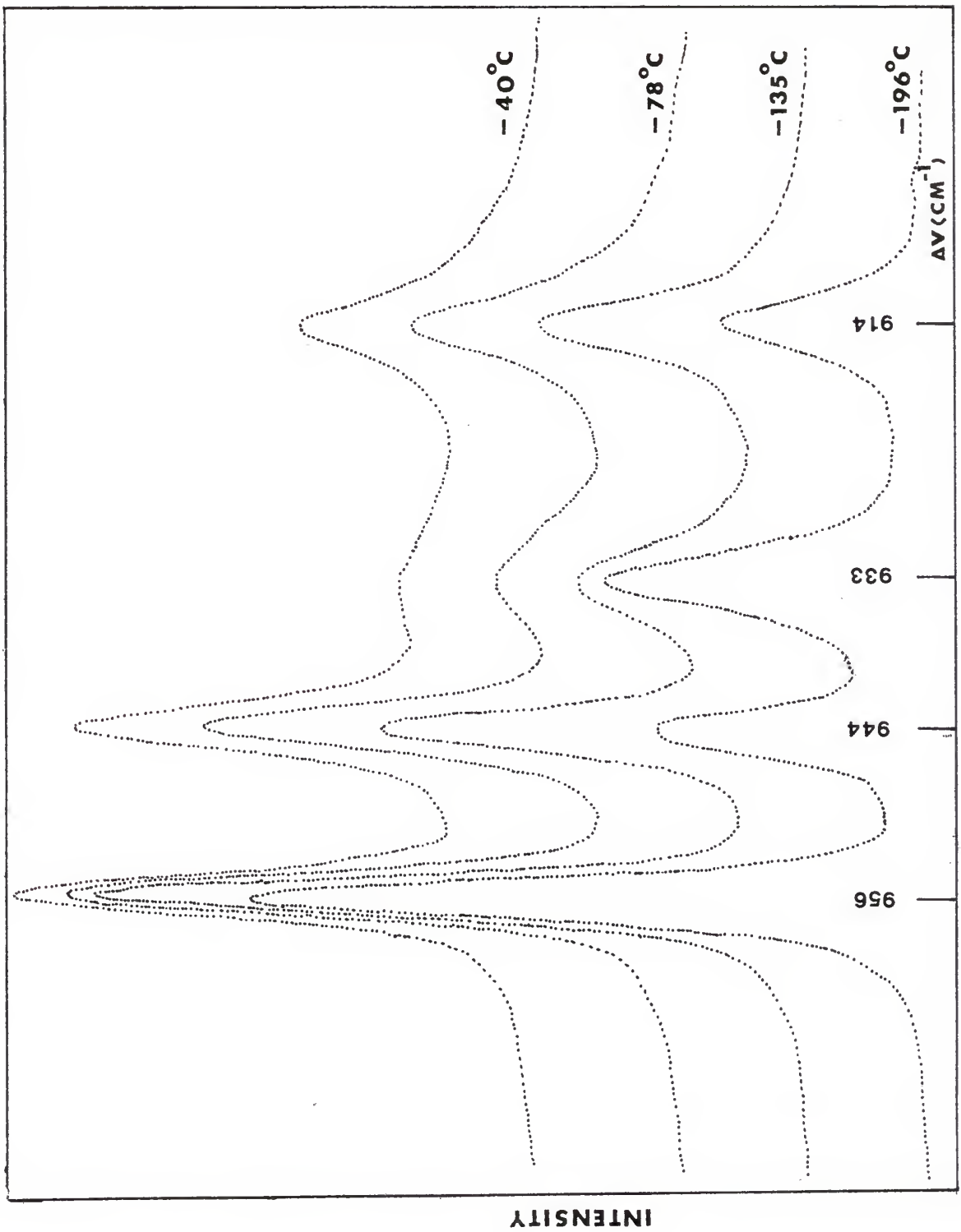
EXPLANATION OF FIGURE 21

Effect of Temperature on the Raman Spectrum
of Liquid $CF_2(OF)_2$ in the Range 900-800 cm^{-1}

Spectrometer: Spex Model 14018

Slit Settings: 200 μm at -196 and -78°C

150 μm at -135 and -40°C

Gain: 3 K

Filter: 0.71%

Scan Speed: 0.2 cm^{-1}/sec

Chart Speed: 3 cm/min

Source: Ar^+ Laser at 5145 Å

Power: 300 mW

Temperature: -196, -135, 178 and -40°C

INTENSITY

ΔV(CM⁻¹)

874 867 860 854 837 827

−40°C
−78°C
−135°C
−196°C
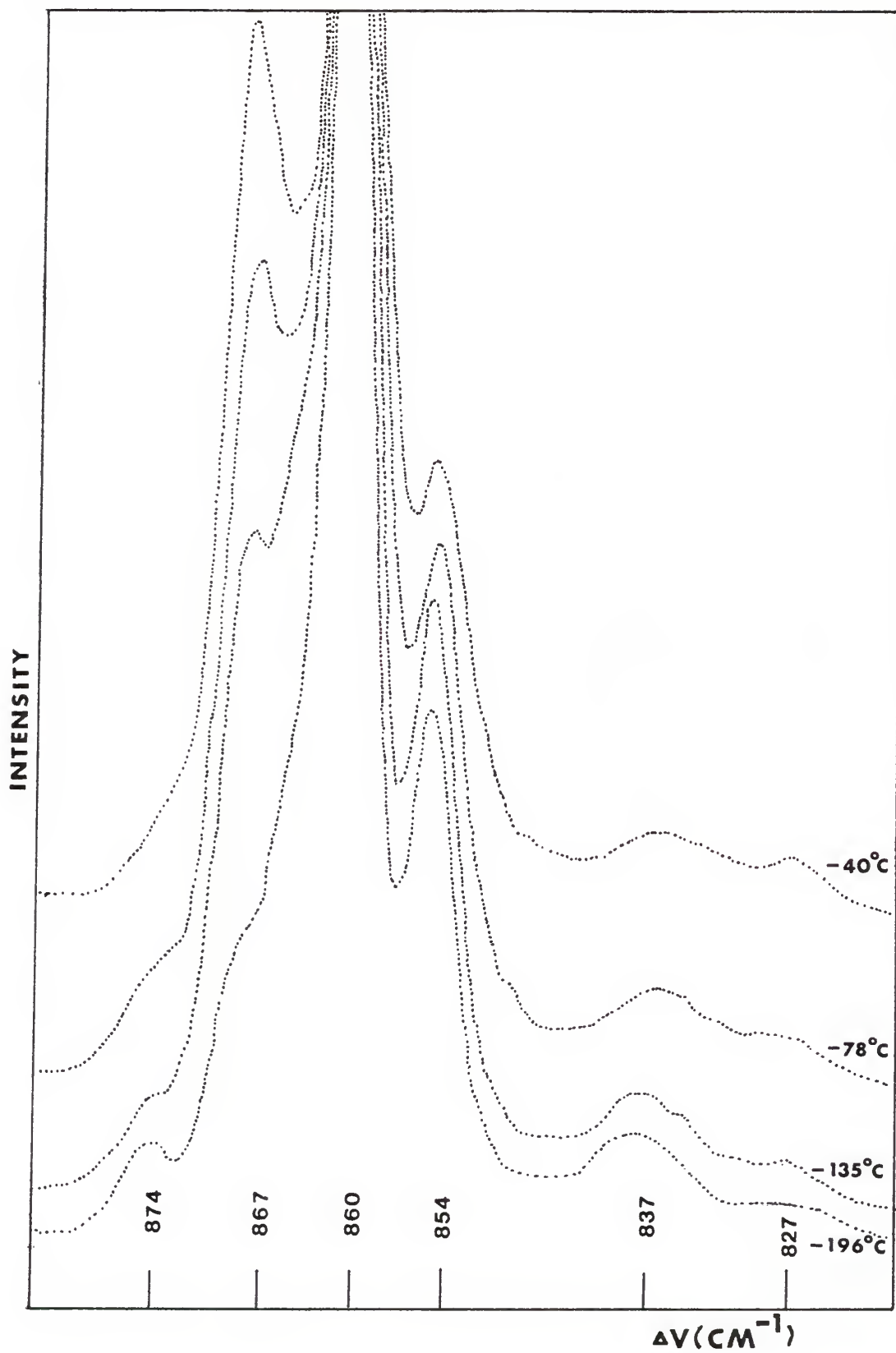
Table 16. Summary of Tentative Assignment for a 2
Conformer Mixture

Low energy conformer			High energy conformer		
Raman liq.[a]	Raman gas[b]	IR gas	Raman liq.[a]	Raman gas[b]	IR gas
	1287.5	1275		1287.5	1275
1240	1246.1	1247	1240	1246.1	1247
1207	1215.6	1207	1207	1215.6	1207
956	956.9	955	944	943.8	942
933	931.0	933Q	914	915.4	916Q
			874		
860	854.9	857	867	863.1	866
854		~850			
837		836.5	827		831
660	657.7	658.5Q	692	687.3	692Q
602 or No	601.9 or No	598 or No	602	601.9	603
524	525?	522.5Q	559	557.3	555Q
437	No?	No,~440?	434	432.5	No
428 or No	No?	426	428	No?	426
304	No?	300Q or No	291	No?	300Q
243	241.1	~240	280	278.9	~280
147			147		
108			108		

a. The liquid Raman frequencies listed are the average values
of the frequencies measured at the four different
temperatures.

b. These frequencies are from reference (19) where the data
are more complete than ours. Our gas phase Raman spectra
in Figure 15 differ in frequency for the most prominent
bands in the 800-1000 cm^{-1} region where we find 958, 945,
867 and 860 cm^{-1} rather than the values 956.9, 943.8,
863.1 and 854.9 cm^{-1} from reference (19) listed above.

From Figures 20 and 21 it can be seen that the relative intensities of the bands at 956, 933, 860 and 854 cm^{-1} decrease when the temperature increases, these bands are classified as belonging to the low energy conformer. The reverse is true for the bands at 944, 914 and 867 cm^{-1}, and they are classified as belonging to the high energy conformer.

A summary of tentative assignments for a 2 conformer or rotational isomer mixture made by taking the available spectroscopic data for comparison is listed in Table 16.

C. Energy Difference between Rotational Isomers

We have concluded that temperature effects in the liquid state could be explained by the presence of the two rotational isomers: high energy conformer or isomer and low energy conformer or isomer.

As seen in Figure 20, relative intensities of the Raman bands at 944 and 956 cm^{-1} vary with temperature, indicating definitely that they belong to different rotational isomers. Since the Raman bands at 944 and 956 cm^{-1} are now assigned to the two different conformers, we can determine the energy difference between the isomers from the temperature dependence of the Raman intensity ratios. It was shown that there seems to be no significant difference in the results obtained whether peak height intensities or band area intensities are used for energy difference calculations (50).

Although the Raman bands at 944 and 956 cm^{-1} partially overlap each other, the peak heights of these two bands were used as a measure of the concentration of the indicated isomer based on the above approximation.

The variations are given as follows:

$$-196^{\circ}C = 77^{\circ}K \qquad -135^{\circ}C = 138^{\circ}K \qquad -78^{\circ}C = 195^{\circ}K$$

$$\frac{I_{956}}{I_{944}} = \qquad 2.53 \qquad\qquad 1.66 \qquad\qquad 1.27$$

The energy difference $\Delta E = E$ (high energy) $- E$ (low energy) was evaluated by the equation (51):

$$\left(\frac{I_{956}}{I_{944}} \right)_{T_1} \bigg/ \left(\frac{I_{956}}{I_{944}} \right)_{T_2} = \exp \left[\frac{\Delta E}{R} \left(\frac{1}{T_1} - \frac{1}{T_2} \right) \right]$$

The values calculated for $T_1 = 77^{\circ}K$ and $T_2 = 138^{\circ}K$, $T_1 = 138^{\circ}K$ and $T_2 = 195^{\circ}K$, and $T_1 = 77^{\circ}K$ and $T_2 = 195^{\circ}K$ were 146, 251, and 174 cal/mole, respectively. Since the data at $138^{\circ}K$ were recorded with a different slit setting and since $77^{\circ}K$ and $195^{\circ}K$ are the most widely separated temperatures below the boiling point of $CF_2(OF)_2$ ($-64^{\circ}C = 209^{\circ}K$), $\Delta E = 174$ cal/mole is probably the most reliable value. The data from $-40^{\circ}C$ was not used for fear of possible vaporization during the recording of the spectrum. An analogous calculation using the 867 and 860 cm^{-1} bands gave 202, 326, and 235 cal/mole, but these values should be less reliable due to more serious overlap between the 867 and 860 cm^{-1} bands than between the

944 and 956 cm^{-1} bands (see Figures 20 and 21). Since a lot of approximations are involved in the calculation, it can only be concluded that energy difference between the two isomers must be quite small and probably is of the order of 100-300 cal/mole.

D.   Suggestions for Future Work

The experimental results presented here demonstrate that the liquid Raman data can be interpreted in terms of an equilibrium mixture of two rotational isomers over the liquid range of $CF_2(OF)_2$ (b. p. $-64^\circ C$) down to near $-196^\circ C$. Other measurements that might be informative include the following: infared and Raman spectra of the pure solid and the solid isolated in an argon matrix, very low temperature F-19 NMR spectra of the liquid, Raman spectra of the liquid with accurate depolarization ratio measurements, and microwave spectra of the gas phase.

If a crystalline solid phase will form below $-196^\circ C$ or if a solid may be isolated in an argon matrix, there may be so little of the high energy isomer present that it will make a negligible contribution to the IR and Raman spectra. Then the fundamentals due to the low energy isomer might be conclusively identified.

If the rate of rotation from one isomer to the other can be slowed sufficiently the F-19 NMR signals will be split into signals for each isomer and the chemical shifts and coupling

constants of each isomer might be obtained. These data might assist in establishing the structure of each isomer.

If one could correctly identify all the depolarized bands in the Raman spectrum of the liquid, then the data in this work would indicate how many depolarized bands each isomer has. Such information might allow one or both isomers to be assigned to the proper point group.

Recently, microwave spectroscopy has been used to identify rotational isomers (52). The gas phase Raman spectrum of $CF_2(OF)_2$ near room temperature in Figure 15 suggests that the two isomers are present in about equal concentrations since the gas phase analogues of the 867 and 860 cm^{-1} bands in the liquid have about the same intensity. Consequently, it might be possible to assign lines to both isomers and obtain structural data for both isomers.

LITERATURE CITED

1. I. W. Levin and R. A. R. Pearce, in <u>Vibrational</u> <u>Spectra</u> <u>and</u> <u>Structure</u>, <u>Vol. 4</u>, (J. R. Durig, ed.), Elsevier Scientific, Amsterdam, 1975, p. 101.

2. C. J. Hoffman, Chem. Rev., <u>64</u>, 91 (1964).

3. C. J. Schack and W. Maya, J. Am. Chem. Soc., <u>91</u>, 2902 (1969).

4. P. M. Wilt and E. A. Jones, J. Inorg. Nucl. Chem., <u>30</u>, 2933 (1968).

5. R. R. Smardzewski and W. B. Fox, J. Fluoro. Chem., <u>6</u>, 417 (1975).

6. P. Buckley and J. P. Weber, Can. J. Chem., <u>52</u>, 942 (1974).

7. C. J. Marsden, D. D. DesMarteau, and L. S. Bartell, Inorg. Chem., <u>16</u>, 2359 (1977).

8. Ajit S. Manocha, M. S. Thesis, Kansas State University, Manhattan, Kansas (1978).

9. E. B. Wilson, Jr., J. C. Decius, and P. C. Cross, <u>Molecular</u> <u>Vibrations</u>, McGraw-Hill, New York, 1955.

10. J. H. Schachtschneider, "Vibrational Analysis of Polyatomic Molecules. V and VI", Tech. Rept. Nos. 231-64 and 57-65, respectively, Shell Development Co., Houston, Texas.

11. K. B. Kellog and G. H. Cady, J. Am. Chem. Soc., <u>70</u>, 3986 (1948).

12. R. T. Lagemann, E. A. Jones, and P. J. H. Woltz, J. Chem. Phys., <u>20</u>, 1768 (1952).

13. F. P. Diodati and L. S. Bartell, J. Mol. Structure, <u>8</u>, 395 (1971).

14. D. D. DesMarteau, Kansas State University, private communication.

15. D. E. Gould, L. R. Anderson, D. E. Young, and W. B. Fox, Chem. Commun., 1564 (1968).

16. M. Lustig, A. R. Pitochelli, and J. K. Ruff, J. Am. Chem. Soc., $\underline{89}$, 2841 (1967).

17. I. U. P. A. C., Tables of Wavenumbers for the Calibration of Infrared Spectrometers, Butterworth, Wahington, D. C. 1961.

18. C. W. Brown, A. G. Hopkins, and F. P. Daly, Appl. Spectry., $\underline{28}$, 194 (1974).

19. R. R. Smardzewski and W. B. Fox, U. S. Naval Research Laboratory, Washington, D. C. 20375, private communication to Dr. D. D. DesMarteau.

20. J. C. Decius, J. Chem. Phys., $\underline{17}$, 1315 (1949).

21. John R. Ferraro and Joseph S. Ziomek, Introductory Group Theory, 2nd Ed. Plenum Press, New York, 1975.

22. J. H. Schachtschneider and R. G. Snyder, Spectrochim. Acta, $\underline{19}$, 117 (1963).

23. D. E. Mann, T. Shimanouchi, J. H. Meal, and L. Fano, J. Chem. Phys., $\underline{27}$, 43 (1957).

24. W. T. King, I. M. Mills, and B. L. Crawford, Jr., J. Chem. Phys., $\underline{27}$, 455 (1957).

25. J. Overend and J. R. Scherer, J. Chem. Phys., $\underline{32}$, 1289 (1960).

26. T. Shimanouchi and I. Suzuki, J. Chem. Phys., $\underline{42}$, 296 (1965).

27. L. Pierce, N. Di Cianni, and R. Jackson, J. Chem. Phys., $\underline{38}$, 730 (1963).

28. Y. Morino and S. Saito, J. Mol. Spectry., 19, 435 (1966).

29. P. N. Noble and G. C. Pimentel, Spectrochim. Acta, $\underline{24A}$, 797 (1968).

30. J. F. Ogilvie, Canad. J. Spectry., $\underline{19}$, 171 (1974).

31. M. M. Rochkind and G. C. Pimentel, J. Chem. Phys., $\underline{42}$, 1361 (1965).

32. B. Beagley, A. H. Clark, and D. W. J. Cruickshank, Chem. Comm., 458 (1966).

33. G. E. Herberich, R. H. Jackson, and D. J. Millen, J. Chem. Soc. (A), 336 (1966).

34. K. O. Christe, C. J. Schack, and E. C. Curtis, Inorg. Chem., 10, 1589 (1971).

35. J. D. Witt and R. M. Hammaker, J. Chem. Phys., 58, 303 (1973).

36. R. N. Dixon, J. Chem. Phys., 31, 258 (1959).

37. E. L. Saier, L. R. Cousins, and M. Basila, J. Phys. Chem., 66, 232 (1962).

38. W. G. Fateley, I. Matsubara, and R. E. Witkowski, Spectrochim. Acta, 20, 1461 (1964).

39. T. Shimanouchi, Tables of Molecular Vibrational Frequencies, Consolidated Volume, NSRDS-NBS-39 (National Bureau of Standards, Washington, D. C., 1972), p. 22.

40. G. M. Begun, and W. H. Fletcher and D. F. Smith, J. Chem. Phys., 42, 2236 (1965).

41. H. Selig, H. H. Claassen, and J. H. Holloway, J. Chem. Phys., 52, 3517 (1970).

42. W. G. Fateley and F. A. Miller, Spectrochim. Acta, 17, 857 (1961).

43. W. G. Fateley and F. A. Miller, Spectrochim. Acta, 18, 977 (1962).

44. W. G. Fateley, F. A. Miller, and R. E. Witkowski, Technical Report AFML-TR-66-408, Air Force Materials Laboratory, Wright-Patterson Air Force Base, Ohio 45433.

45. P. G. Thompson, "Oxygen Fluorides and Hypofluorites", The Fluorine Symposium of the Inorganic Division of the American Chemical Society, Ann Arbor, Mich., June 27, 1966.

46. P. Thompson, J. Am. Chem. Soc., 89, 1811 (1967).

47. F. A. Hohorst and J. M. Shreeve, J. Am. Chwm. Soc., 89, 1809 (1967).

48. R. W. Mitchell and J. A. Merrit, J. Mol. Spectry., 24, 128 (1967).

49. P. J. D. Park, R. A. Pethrick and B. H. Thomas, in *Internal Rotation in Molecules*, (W. J. Orville Thomas ed.), John Wiley & Sons, London, 1974, p.83.

50. H. J. Bernstein, J. Chem. Phys., 17, 258 (1949).

51. A. Langeseth and H. J. Bernstein, J. Chem. Phys., 8, 410 (1940).

52. N. S. True and R. K. Bohn, J. Phys. Chem., 81, 1667, 1671 (1977).

53. A. Müller and B. Krebs, J. Mol. Spectroscopy, 24, 180 (1967); B. Krebs, A. Müller, and A. Fadini, J. Mol. Spectroscopy, 24, 198 (1967); J. L. Duncan and I. M. Mills, Spectrochim Acta, 20, 1089 (1964).

54. A. Ruoff, H. Burger, and S. Biedermann, Spectrochim. Acta, 27A, 1359 (1971); R. W. Kirk and P. M. Wilt, J. Mole. Spectroscopy, 58, 102 (1975).

ACKNOWLEDGMENT

A considerable portion of one's destiny is molded by those people with whom he is associated. While one must accept the ultimate responsibility for the realization of his objectives, it is obvious that they can not be achieved without the assistance and encouragement of others.

In appreciation of this, the author would like to extend his sincere gratitude to Professor R. M. Hammaker for his invaluable contributions to this work. Also for his patience, valuable discussion and all his help during the course of this study, the author is deeply appreciative.

The author is deeply indebted to Professors W. G. Fateley and D. D. DesMarteau for their incomparable guidance and assistance over the year when Dr. Hammaker was abroad. Also the help from the Flourine Chemistry Laboratory of Kansas State University deserves the author's special thanks.

Last but not least, the author wishes to convery special praise to his wife, Fen. Without her love and understanding, none of this work would have been accomplished.

VITA

The author was born on February 21, 1950, in Yun-Lin, Taiwan, Republic of China. He obtained his B.S. degree in Chemistry from National Taiwan University in June, 1972. He began graduate study at Kansas State University in August, 1974. He is a member of Phi Lambda Upsilon.

STUDIES IN VIBRATIONAL SPECTROSCOPY

I. NORMAL COORDINATE ANALYSIS OF CF_3OF AND CF_3OCl

II. RAMAN SPECTRA OF $CF_2(OF)_2$ AS A FUNCTION OF
    TEMPERATURE

by

JENG-CHUNG KUO

B.S., National Taiwan University, 1972

_____

AN ABSTRACT OF A MASTER'S THESIS

Submitted in partial fulfillment of the

requirements for the degree

MASTER OF SCIENCE

Department of Chemistry

KANSAS STATE UNIVERSITY
Manhattan, Kansas

1978

I. NORMAL COORDINATE ANALYSIS OF CF_3OF AND CF_3OCl

Raman and infrared data previously obtained in this laboratory are used to perform a normal coordinate analysis on CF_3OF and CF_3OCl. All infrared and Raman bands below 1400 cm^{-1} have been assigned under C_s symmetry. Both the fundamental and the first overtone of the CF_3 torsion in both CF_3OF and CF_3OCl have been observed. The two CF_3 rocking modes of both CF_3OF and CF_3OCl appear to be well separated in frequency. The barriers to internal rotation of the CF_3 group are 4.4 and 4.2 kcal/mole in CF_3OF and CF_3OCl, respectively. An unexpected band near 548 cm^{-1} in the Raman spectrum of liquid CF_3OCl near $77^{O}K$ is tentatively assinged to the stretching of the chlorine to chlorine bond of molecular chlorine in a complex with CF_3OCl.

II. RAMAN SPECTRA OF $CF_2(OF)_2$ AS A FUNCTION OF TEMPERATURE

Raman and infrared data have been obtained for $CF_2(OF)_2$. The large number of bands in the Raman spectrum of the liquid have been interpreted in terms of a mixture of two rotational isomers or conformers. Raman spectra of liquid $CF_2(OF)_2$ at -196, -135, -78, and -40°C have been used to assign the observed Raman and infrared bands to a high energy conformer and low energy conformer. Using peak heights of strong Raman bands between 800 and 1000 cm^{-1}, the energy separation between the two conformers is estimated to be in the range 100 to 300 cal/mole.